BIOLOGY OF REPRODUCTION (2013) **89**(2):37, 1–17
Published online before print 19 June 2013.
DOI 10.1095/biolreprod.113.110783

Subcellular Localization of Selectively Permeable Aquaporins in the Male Germ Line of a Marine Teleost Reveals Spatial Redistribution in Activated Spermatozoa[1]

François Chauvigné,[3] Mónica Boj,[3] Sebastiano Vilella,[4] Roderick Nigel Finn,[5,6] and Joan Cerdà[2,3]

[3]*Institut de Recerca i Tecnologia Agroalimentàries (IRTA)-Institut de Ciències del Mar, Consejo Superior de Investigaciones Científicas (CSIC), Barcelona, Spain*
[4]*Laboratory of Comparative Physiology, Department of Biological and Environmental Sciences and Technologies, University of Salento, Lecce, Italy*
[5]*Institute of Biology, Bergen High Technology Centre, University of Bergen, Bergen, Norway*
[6]*Institute of Marine Research, Nordnes, Bergen, Norway*

ABSTRACT

In oviparous vertebrates such as the marine teleost gilthead seabream, water and fluid homeostasis associated with testicular physiology and the external activation of spermatozoa is potentially mediated by multiple aquaporins. To test this hypothesis, we isolated five novel members of the aquaporin superfamily from gilthead seabream and developed paralog-specific antibodies to localize the cellular sites of protein expression in the male reproductive tract. Together with phylogenetic classification, functional characterization of four of the newly isolated paralogs, Aqp0a, -7, -8b, and -9b, demonstrated that they were water permeable, while Aqp8b was also permeable to urea, and Aqp7 and -9b were permeable to glycerol and urea. Immunolocalization experiments indicated that up to seven paralogous aquaporins are differentially expressed in the seabream testis: Aqp0a and -9b in Sertoli and Leydig cells, respectively; Aqp1ab, -7, and -10b from spermatogonia to spermatozoa; and Aqp1aa and -8b in spermatids and sperm. In the efferent duct, only Aqp10b was found in the luminal epithelium. Ejaculated spermatozoa showed a segregated spatial distribution of five aquaporins: Aqp1aa and -7 in the entire flagellum or the head, respectively, and Aqp1ab, -8b, and -10b both in the head and the anterior tail. The combination of immunofluorescence microscopy and biochemical fractionation of spermatozoa indicated that Aqp10b and phosphorylated Aqp1ab are rapidly translocated to the head plasma membrane upon activation, whereas Aqp8b accumulates in the mitochondrion of the spermatozoa. In contrast, Aqp1aa and -7 remained unchanged. These data reveal that aquaporin expression in the teleost testis shares conserved features of the mammalian system, and they suggest that the piscine channels may play different roles in water and solute transport during spermatogenesis, sperm maturation and nutrition, and the initiation and maintenance of sperm motility.

aquaporin, mitochondria, motility, sperm, spermatogenesis, teleost

INTRODUCTION

Water transport during gametogenesis is an essential physiological process associated not only with successful reproduction of vertebrates [1–3], but also with their adaptive evolution in the oceanic environment [4]. While several studies have highlighted the key role played by transmembrane water channels (aquaporins) during oocyte hydration of marine teleosts [5], the function of aquaporins in the reproductive physiology of the male germ line of fishes remains virtually unknown. This is despite the fact that the majority of marine teleosts are oviparous and the hyperosmotic seawater to which the ejaculate is exposed is a key signal in sperm motility activation [1, 6].

To date, only a single study has shown that aquaporin proteins are expressed in the spermatozoa of a marine teleost, the gilthead seabream (*Sparus aurata*) [7]. This study revealed that the water-specific channel aquaporin-1aa (Aqp1aa) and the glycerol-, urea-, and water-transporting channel Aqp10b are both present in the head and flagellum of ejaculated spermatozoa, and that mercury, an inhibitor of Aqp1aa and -10b water transport [7–10], blocks sperm motility in seawater [7]. These findings suggest that the proposed activation of adenylyl cyclase and the initiation of sperm motility that coincides with water efflux from spermatozoa exposed to seawater [6, 11] may be mediated via aquaporins.

A role for multiple classes of aquaporins in the male reproductive physiology of fishes can be further inferred from data available for mammals. For example, in the somatic cells of the mammalian testis, AQP0 and -9 are expressed in the Leydig cells [12–14], while AQP0 and -8 are expressed in Sertoli cells, where they are suggested to facilitate water transport across the blood-testis barrier [12, 15–17]. AQP1, -9, and -10 have also been found in the epithelial cells of the efferent duct, where they are assumed to mediate water reabsorption [12, 13], whereas AQP1, -3, and -9 in the epididymis may help to maintain the composition of the seminal fluid, ensuring proper sperm maturation [12, 13, 18, 19]. In the germ line, the differentiating germ cells may express AQP7, -8, and -11, with AQP8 found in all spermatogenic cell types [20–23]. Subcellular localization studies have further shown that AQP7 is commonly localized in the plasma membrane and, to a weaker extent, in the cytoplasm of round and elongated spermatids [21, 23, 24], whereas AQP11 is

[1]Supported by the Spanish Ministry of Science and Innovation (MICINN; AGL2010-15597 to J.C.), with additional financial support from the Research Council of Norway (204813/F20 and 224816/E40 to R.N.F.), and from the Ministry of Agriculture and Aquaculture of the Puglia Region (Italy) under the program between the Region of Puglia and the University of Salento (to S.V.). F.C. and M.B. were supported by a postdoctoral (Juan de la Cierva Programme) and predoctoral (FPI) fellowship, respectively, from MICINN.
[2]Correspondence: Joan Cerdà, IRTA-Institut de Ciències del Mar (CSIC), Passeig marítim 37–49, 08003 Barcelona, Spain.
E-mail: joan.cerda@irta.cat

Received: 14 May 2013.
First decision: 11 June 2013.
Accepted: 17 June 2013.

eISSN: 1529-7268 http://www.biolreprod.org
ISSN: 0006-3363

found in the caudal cytoplasm of elongating spermatids. Although the function of AQP11 in the testis is not yet known, because knockout mice die of renal failure before puberty [25], it has been suggested that this channel could be involved in the release of the residual body during spermiogenesis [22]. AQP7, -8, and -11, together with AQP3, are also present in spermatozoa [26–28], but they are spatially separated in the head and along the sperm flagellum. In spermatozoa, AQP3 has been suggested to play a role in osmoadaptation and migration [28], AQP7 in sperm energy metabolism and motility [21, 26], and AQP8 in spermatozoan volume regulation in response to osmotic challenge [27].

Based on the above information available from mammalian models and the initial studies in gilthead seabream [7, 29], together with recent observations that mRNAs encoding different classes of aquaporins are expressed in the testes of several species of teleosts [30, 31], it is plausible that multiple water channels have regulatory roles associated with the testicular homeostasis, spermatogenesis, spermiogenesis, and sperm physiology of fishes. Compared to mammals, however, teleosts are known to harbor a larger repertoire of aquaporins due to the retention in the genome of two, or in some cases three, orthologs of the human counterparts [30, 32, 33]. Given that some teleost aquaporins, such as Aqp1ab expressed in the female germ line, are evolving more rapidly than the mammalian counterparts [34], it remains to be established whether the increased copy number of piscine aquaporins have evolved redundant or novel functions associated with the male reproductive biology of teleosts.

In the present work, therefore, we isolated and functionally characterized five additional members of the aquaporin superfamily from the gilthead seabream. By combining immunofluorescence microscopy and immunohistochemistry using paralog-specific antibodies as well as biochemical fractionation of spermatozoa, we show for the first time in a nonmammalian vertebrate that up to seven classes of aquaporins are differentially expressed during spermatogenesis and spermiogenesis, with several paralogs being spatially redistributed in the plasma membrane upon the activation of sperm motility.

MATERIALS AND METHODS

Animals and Sperm Collection

Adult gilthead seabream males and females were raised in captivity at Institut de Recerca i Tecnologia Agroalimentàries (IRTA) aquaculture facilities in San Carlos de la Rápita (Tarragona, Spain) and transported to the laboratory. For the present experiments, the adults were maintained in 12 000-L tanks under natural conditions of photoperiod and temperature and fed three times a week with a mixture of pellets and squid. In the autumn and winter (November and February, respectively), milt was recovered from males sedated with 500 ppm of phenoxyethanol (Sigma-Aldrich, St. Louis, MO). The procedure involved the application of soft pressure to the abdominal area and removal of sperm from the gonopore with a syringe in order to avoid contamination with seawater or urine. The sperm sample was transferred to an Eppendorf tube and kept on ice until further analysis. Some males were euthanized by decapitation, and samples of testis and other tissues were immediately frozen in liquid nitrogen and stored at -80°C until RNA and protein extraction. Additional pieces of the testis and efferent duct were taken for histological analysis and immunohistochemistry. Procedures relating to the care and use of animals were approved by the Ethics Committee from IRTA in accordance with the European Union regulations.

Cloning of Gilthead Seabream Aquaporin cDNAs

Aquaporin-encoding cDNAs were isolated by RT-PCR. Total RNA was extracted from different tissues, including testis and sperm, using the RNeasy Minikit (Qiagen GmbH, Hilden, Germany) and treated with DNAse using the RNase-Free DNase kit (Qiagen) following the manufacturer's instructions. Total RNA (5 μg) was reverse transcribed using 0.5 μg oligo(dT)$_{17}$, 1 mM deoxynucleotide triphosphates (dNTPs), 40 IU RNAse inhibitor (Roche Applied Science, Mannheim, Germany), and 10 IU SuperScript II Reverse Transcriptase enzyme (Life Technologies Corp., Carlsbad, CA) for 1.5 h at 42°C. The PCR was carried out with 0.5–2 μl of the RT reaction in a final volume of 50 μl containing 1× PCR buffer plus Mg^{2+}, 0.2 mM dNTPs, 1 IU of Taq polymerase (Roche), and 1 μM of primers. Degenerated primers were used to amplify products for Aqp0a (forward = 5′-GTGGGAGYTSMRNTCNATGWHBTTYTGG-3′ and reverse = 5′-GCMGGRGCRAAVGAYCKNGCDGGGTTCA-3′), Aqp3a (forward = 5′-CTCATCCTKGTRTGTTYGG-3′ and reverse = 5′-CCRGARTTRAAGCCCATRGA-3′), Aqp7 (forward = 5′-GTBGCBATGGGDRTNCAYGTTG-3′ and reverse = 5′-GCVCCYAAAAMTCCTCCRAT-3′), and Aqp9b (forward = 5′-AACCCBGCBGTBTCYYTGGCBATGGT-3′ and reverse = 5′-CCNRCMACHGGRAYCCACCACCAG-3′). Reactions were amplified using one 5-min cycle of 95°C; then 35 cycles of 95°C for 30 sec, 50°–58°C (depending on primer Tm) for 30 sec, and 72°C for 1 min; and a final 7-min elongation at 72°C. The products were cloned into the pGEM-T Easy Vector (Promega) and sequenced by BigDye Terminator v3.1 cycle sequencing on ABI PRISM 377 DNA analyzer (Applied Biosystems [Life Technologies]). Full-length cDNAs for Aqp0a, -3a, -7, and -9b were amplified using 3′- and 5′-RACE kits (Life Technologies Corp.), followed by a final amplification using the Easy-ATM High-Fidelity PCR cloning enzyme (Agilent Technologies, Santa Clara CA). A partial cDNA encoding seabream Aqp4a carrying the 3′UTR was isolated by 3′-RACE using specific primers designed based on an available sequence (GenBank accession number FM146410). The nucleotide sequences of gilthead seabream Aqp0a, -3a, -4a, -7, and -9b were deposited in GenBank under accession numbers KC589385, KC788197, KC788198, KC589386, and KC589387, respectively.

Phylogenetic Analyses

Phylogenetic analyses of the gilthead seabream sequences were conducted using Bayesian and maximum-likelihood protocols as described previously [4, 32]. Two data sets consisting of full-length classical aquaporins (Aqp0, -1, and -4) and aquaglyceroporins (Aqp3, -7, -9, and -10) were constructed from 228 vertebrate orthologs obtained via BLAST from nonredundant protein, expressed sequence tags, and whole genome databases (NCBI GenBank, Ensembl). To improve the resolution and to validate the novel teleost subclusters, several sequences (see Supplemental Table S1; all Supplemental Data are available online at www.biolreprod.org) were assembled from whole-genome shotgun contigs as described by Zapater et al. [34]. Deduced amino acid sequences of each data set were aligned using MAFFT version 7.037b [35] and converted to codon alignments using PAL2NAL [36] prior to phylogenetic analyses. For Bayesian analyses, 5 million MCMC generations were run with aamodel = mixed for amino acid alignments and nucmodel = 4by4 with nst = 2 for the codon alignments. All runs were examined for convergence using Tracer version 1.5 (www.beast.bio.ed.ac.uk/Tracer) and majority rule consensus trees summarized with a burnin of 3500.

RT-PCR Analysis of Aquaporin Gene Expression

Extraction of total RNA from testis and sperm and cDNA synthesis was carried out as described above. PCR reactions were carried out with 1 μl of cDNA reaction in a volume of 50 μl containing 1× PCR buffer plus Mg^{2+}, 0.2 mM dNTPs, 1 IU Taq polymerase, and 0.05–0.4 μM of aquaporin isoform-specific oligonucleotide primers (Supplemental Fig. S1A). When possible, oligos were designed to flank one intron. Reactions were amplified using one cycle at 95°C for 2 min; 40 cycles at 95°C for 30 sec, 60°–62°C (depending on primer Tm) for 30 sec, and 1 min at 72°C; and a final 7-min elongation at 72°C. Genomic DNA and plasmids containing the aquaporin cDNAs were used as controls.

Functional Analysis in *Xenopus laevis* Oocytes

Full-length aquaporin cDNAs were subcloned into the pT7Ts vector for ex vivo expression in *X. laevis* oocytes. The cRNAs for microinjection of oocytes were synthesized with T7 RNA polymerase (Roche) from *Xba*I or *Sal*I-linearized plasmids (depending on the restriction sites identified in the aquaporin sequences). Isolation of stage V oocytes and microinjection were performed as previously described [37]. Oocytes were transferred to modified Bart Solution (MBS; 88 mM NaCl, 1 mM KCl, 2.4 mM $NaHCO_3$, 0.82 mM $MgSO_4$, 0.33 mM $Ca(NO_3)_2$, 0.41 mM $CaCl_2$, 10 mM HEPES, and 25 μg/ml gentamycin; pH 7.5) and injected with 50 nl of distilled water (negative control) or 50 nl of water solution containing 1 (Aqp0a and -9b), 5 (Aqp8b), or 10 ng (Aqp7) of cRNA. One day after injection, oocytes were manually defolliculated and subsequently maintained in MBS at 18°C.

The osmotic water permeability (P_f) was determined 2 days after injection at room temperature. Oocytes were transferred to 10-fold-diluted MBS (20 mOsmol), and oocyte swelling was recorded by video microscopy using serial images at 2-sec intervals during the first 20 sec using a Nikon Color view video camera coupled to a stereomicroscope (SMZ1000; Nikon Corp., Tokyo, Japan). The P_f values were calculated by taking into account the time-course changes in relative oocyte volume [$d(V/V_0)/dt$], the molar volume of water ($V_W = 18$ cm^3/ml), and the oocyte surface area (S) using the formula $V_0[d(V/V_0)/dt]/[SV_W(Osm_{in} - Osm_{out})]$. The surface area of the oocyte was considered to be nine times the apparent area due to membrane folding [38]. Inhibition of water transport by mercury was investigated by incubating oocytes in MBS containing 0.1 mM $HgCl_2$ for 15 min before and during the swelling assays. The reversibility of the mercury inhibition was determined by rinsing the same oocytes three times with fresh medium and incubating further with 5 mM β-mercaptoethanol for 15 min prior to the swelling assays.

Glycerol and urea uptake of *X. laevis* oocytes expressing aquaporins were determined under isotonic conditions. Groups of 10 oocytes injected with water or 25 ng aquaporin cRNA were incubated at room temperature in 200 μl of isotonic MBS containing 5 μM (20 μCi) of [1,2,3-^{3}H]glycerol (50 Ci/mmol) or [^{14}C]urea (58 mCi/mmol) (American Radiolabelled Chemicals Inc., St Louis, MO) and cold glycerol or urea at 1 mM final concentration. After 10-min exposure to radioactive compounds (including zero time for subtraction of the signal from externally bound solute), oocytes were washed rapidly in ice-cold MBS three times, and individual oocytes were dissolved for 1 h in 400 μl of 10% SDS before scintillation counting.

Antibodies

Antisera were raised in rabbits against synthetic peptides corresponding to the C-terminus amino acid residues of Aqp0a (CAEGQQETRGEPIELKTQAL), Aqp7 (CLVEEETAPLGKKENI), and Aqp9b (CPEKQEEKNVQDKYEI) (AbBcn S.L., Barcelona, Spain), as well as of Aqp8b (LGDRKMRLILK; GenBank accession no. DQ889225; Agrisera AB, Vännäs, Sweden), with the predicted initiation codon (methionine, ATG) designated as residue 1. All antisera were affinity purified against the synthetic peptides. Previously characterized antibodies against gilthead seabream Aqp1aa [9], Aqp1ab [39], and Aqp10b [7] were also employed.

Activation of Sperm Motility and Computer-Assisted Sperm Analysis

Two 50-μl aliquots of each sperm sample were gently centrifuged (1200 × *g*, 10 min, 4°C), the seminal plasma was discarded, and the pellet was frozen in liquid nitrogen and kept at -80°C for protein extraction. An additional sperm aliquot was diluted 1:100 with nonactivating medium (NAM; in mg/ml: 3.5 NaCl, 0.11 KCl, 1.23 $MgCl_2$, 0.39 $CaCl_2$, 1.68 $NaHCO_3$, 0.08 glucose, 1 bovine serum albumin [BSA]; pH 7.7), further activated by dilution 1:10 in filtered seawater, and loaded under a cover slip before being video-recorded for 1 sec. Videotapes were analyzed using the Integrated Semen Analysis System software (ISAS version 1; Proiser, Valencia, Spain). For each sperm sample, at least two aliquots were analyzed. Only sperm samples with at least 75% motile spermatozoa were used for further experiments.

Protein Extraction from Testis and Sperm

Testis and sperm samples were processed for protein extraction as previously described [7]. Testis biopsies were dissociated with a glass dounce homogenizer in lysis buffer (50 mM Tris-HCl [pH 7.4], 1% Triton X-100, 0.25% sodium deoxycholate, 150 mM NaCl, 1 mM ethylenediaminetetraacetic acid [EDTA], 1 mM PMSF, protease inhibitors [EDTA-free Protease Inhibitor Cocktail Tablets; Roche], 1 mM Na_3VO_4, and 1 mM NaF) and centrifuged at 18 000 × *g* for 15 min at 4°C. Nonactivated (NAM-diluted) and seawater-activated spermatozoa were recovered by centrifugation at 1200 × *g* for 10 min at 4°C, and pellets were treated as above. One aliquot of testis and sperm supernatants was removed to determine the protein concentration with the Bio-Rad Protein Assay kit (Bio-Rad Laboratories Inc., Hercules, CA). The rest of the supernatants were mixed with 4× Laemmli sample buffer, frozen in liquid nitrogen, and stored at -80°C until Western blot analysis. To determine the phosphorylation state of the proteins, some sperm samples were homogenized directly in NEBuffer 3 (New England Biolabs Inc., Ipswich, MA), and a protein extract (60 μg) was digested with 1 U/μg protein of calf intestine alkaline phosphatase (CIP; New England Biolabs Inc.) for 1–2 h at 37°C.

Plasma Membrane Purification of Intact Spermatozoa, Head, and Flagellum

Plasma membrane extraction from sperm was carried out following an adapted protocol from de Curtis et al. [40] and Labbé and Loir [41]. For total sperm, activated and nonactivated spermatozoa were recovered as above; homogenized in a buffer containing 20 mM Tris-HCl (pH 7.8), 3 mM $MgCl_2$, 0.25 M sucrose, and protease inhibitors; and centrifuged at 1000 × *g* for 20 min at 4°C. The supernatant was centrifuged again at 100 000 × *g* for 45 min at 4°C, and the pellet was resuspended in PBS containing protease inhibitors. Protein concentration was determined, and the rest of the extract was mixed with 4× Laemmli sample buffer and stored at -80°C.

Isolation of spermatozoa heads and flagella was performed following the methods described in Zilli et al. [29] and Beirão et al. [42]. Briefly, sperm samples (0.25 ml) were activated in seawater or diluted in NAM, and centrifuged at 4000 × *g* for 15 min at 4°C. Pellets were washed once with 5 ml of 1% NaCl, and finally diluted 1:30 with 1% NaCl. Head and flagellum were separated by passing 10 times through a capillary (0.5 mm diameter) attached to a 20-ml syringe. The proper separation of heads and flagella was verified under a microscope. The total suspension (heads plus flagella) was centrifuged at 5000 × *g* for 15 min at 4°C. The pellet was resuspended in 8 ml of 1% NaCl, placed on top of a sucrose gradient (2 M, 1.5 M, 1 M, and 0.5 M), and centrifuged at 28 000 × *g* for 45 min at 4°C. Heads and flagella were recovered separately with a micropipette from the 2 M–1.5 M interface and the top of the gradient, respectively. Samples were diluted in a final volume of 40 ml in 1% NaCl, and the heads suspension was centrifuged at 3000 × *g* for 20 min at 4°C, while the flagella suspension was centrifuged at 5000 × *g* for 20 min at 4°C. Finally, the plasma membrane fraction from both pellets was isolated as described above.

Western Blotting

Laemmli-mixed protein samples from total testis and sperm (60 μg) and from plasma membrane fractions (40 μg) were denatured at 95°C and subjected to 12% SDS-PAGE. To determine whether some aquaporins were glycosylated, Laemmli samples were treated or not with 10 U/μg protein of N-Glycosidase F (PNGase F; New England Biolabs Inc.) for 3 h at 37°C before electrophoresis. Electrophoresed proteins were blotted onto nitrocellulose membranes (Sigma-Aldrich), and after blocking in 5% nonfat dry milk in TBST (20 mM Tris, 140 mM NaCl, 0.1% Tween; pH 7.6), membranes were incubated overnight at 4°C, with each anti-aquaporin antibody diluted in blocking solution: 1:400 for Aqp1aa, -0a, -7, and -9b antisera; 1:600 for Aqp1ab and -8b antisera; and 1:500 for the Aqp10b antiserum. Bound antibodies were detected with horseradish peroxidase (HRP)-coupled anti-rabbit IgG antibody (1:2000; Rockland Immunochemicals Inc., Gilbertsville, PA), and reactive protein bands were detected using Picomax Sensitive Chemiluminescent HRP Substrate (Rockland Immunochemicals Inc.). For the semiquantitative determination of aquaporin abundance in the spermatozoa plasma membrane during motility activation, the intensity of the aquaporin immunoreactive bands in the plasma membrane fraction of total sperm, head, and flagellum—determined by densitometry using the Quantity-One software (Bio-Rad Laboratories Inc.)—was normalized to that in the total protein fraction. This analysis was carried out on sperm from five different males.

Histology

Testis biopsies were fixed in Bouin solution for 16–24 h, dehydrated, and embedded in paraplast (Sigma-Aldrich). Sections 7 μm thick were stained with hematoxilin and eosin (Sigma-Aldrich), dehydrated, and mounted with Fluka-Eukitt mounting medium (Sigma-Aldrich).

Immunofluorescence Microscopy and Immunohistochemistry on Tissue Sections

For immunofluorescence, testis samples were fixed in 4% paraformaldehyde (PFA), washed, dehydrated, and embedded in paraffin. Sections (7 μm) were then rehydrated in decreasing ethanol solutions and subsequently permeabilized using different protocols depending on the antibody used: 10 min in cold acetone (−20°C) followed by two washes in PBST (0.1% Tween in PBS) and demasking in boiling citrate buffer (10 mM, pH 6) three times for 5 min each, then washing in PBST (Aqp7); or 10 min in PBS containing 0.2% Triton X-100 (Aqp0a, -1aa, -8b, -9b, and -10b) or 0.2% SDS (Aqp1ab). In all cases, sections were blocked in 5% goat serum and 0.1% BSA in PBST for 1 h. Incubation with the antibodies (1:400 for Aqp0a, -1aa, -8b, -9b, and -7 antisera; 1:200 for Aqp1ab and -10b antisera) was performed overnight at 4°C in PBST containing 1% goat serum and 0.1% BSA. A set of slides was incubated with

the antibodies preadsorbed with the respective immunizing peptides as negative controls. After washing, sections were incubated with a secondary Cy3-coupled anti-rabbit IgG sheep antibody for 1 h at room temperature and washed in PBS. The nuclei were counterstained with 4′,6-diamidino-2-phenylindole (DAPI; 1:3000, 3 min in PBS; Sigma-Aldrich) and finally mounted with fluoromount aqueous anti-fading medium (Sigma-Aldrich).

For immunohistochemistry of Aqp10b in the efferent duct, the protocol was the same as above except that sections were incubated with a secondary anti-rabbit IgG HRP-coupled goat antibody for 2 h. The reaction was made visible by using a mixture of 0.06% 3,3′-diaminobenzidine (DAB; Sigma-Aldrich) in 0.05 M Tris-HCl (pH 7.6) and 0.03% hydrogen peroxide for 20 min in the dark. Sections were then rinsed in PBS and counterstained with methylene blue, dehydrated, and mounted with Fluka-Eukitt mounting medium.

Immunofluorescence Microscopy on Spermatozoa

Spermatozoa diluted in NAM and activated with seawater for ~2 min were attached to UltraStick/UltraFrost Adhesion slides (Electron Microscopy Sciences, Hatfield, PA) at room temperature, fixed in 4% PFA for 5 min, and processed for immunofluorescence as described previously. For the visualization of potential colocalization of aquaporins with the mitochondria, NAM-diluted spermatozoa were incubated with 250 ng/ml of the mitochondrion-specific vital dye MitoTracker Red CMXRos (Life Technologies Corp.) for 45 min at room temperature under agitation. The samples were then centrifuged for 10 min at $1200 \times g$, washed twice in NAM, and either activated in seawater or diluted in NAM before immunofluorescence processing. In this case, the secondary antibody used to reveal the reaction was a sheep anti-rabbit fluorescein isothiocyanate-coupled antibody (Sigma-Aldrich). The percentage of spermatozoa showing colocalization of aquaporin and MitoTracker signals (yellow color) in each group was determined on 150 spermatozoa from six males.

Measurement of Fluorescence Intensity in Spermatozoa

Immunofluorescence microscopy images for each aquaporin were acquired with a Zeiss Axio Imager Z1/ApoTome fluorescence microscope (Carl Zeiss Corp., Jena, Germany) using the same fluorescence intensity and exposure for nonactivated and activated spermatozoa. The changes in aquaporin expression in different regions of the spermatozoa were estimated by measuring the mean fluorescence intensity of the immunoreactions in the head and the anterior and posterior tail using the ImageJ software (National Institutes of Health, USA; http://rsb.info.nih.gov/ij/). Color images were split for the different colors (blue [DAPI] to stain nuclei vs. green or red for aquaporin immunostaining) and converted to 8-bit images in gray scale. For the head, the selected area corresponding to the DAPI staining was 0.06 pixels square. The aquaporin fluorescence intensity of the anterior flagellum protruding into the head, the area of which was 0.005 pixels square, was subtracted and added to the anterior tail measurement. In the tail, the fluorescence intensity was measured, for a total of 0.2 pixels square, with 0.04 pixels square corresponding to the most anterior part of the tail and 0.16 pixels square to the posterior region. Mean fluorescence intensities were expressed in arbitrary units, after subtraction of the net fluorescence intensity of the background for the same corresponding area. For each aquaporin, fluorescence was determined for 25–50 activated and nonactivated spermatozoa per male (n = 4–5 males).

Statistics

Data are presented as the mean ± SEM. For all experiments, sperm samples from a minimum of four different males were used. Data were statistically analyzed by the Student *t*-test or by one- or two-way ANOVA, followed by Tukey pairwise comparison. Percentage data that fell between the ranges of 0%–20% or 80%–100% were square-root transformed prior to statistical analyses. $P < 0.05$ was considered statistically significant.

RESULTS

Cloning and Phylogenetic Analysis of Gilthead Seabream Aquaporins

To expand the repertoire of seabream aquaporin transcripts available for experimentation, we first cloned the cDNAs encoding Aqp0a, -3a, -4a, -7, and -9b. Total RNA from different tissues—eye (Aqp0a), gills (Aqp3a), muscle (Aqp4a), and testis (Aqp7 and -9b)—was extracted and used for initial RT-PCR experiments with degenerate oligonucleotide primers to clone partial sequences. By using 5′ and 3′ RACE methods, full-length cDNAs for *aqp0a*, *-3a*, *-7*, and *-9b* were isolated and found to encode proteins of 263, 302, 308, and 288 amino acids, respectively. The deduced amino acid sequences of each of the newly cloned seabream aquaporins contain six predicted transmembrane helices and two NPA boxes that are the hallmark of the membrane integral protein (MIP) superfamily [43]. The only exception was Aqp7, in which Pro is substituted by Ala in the first box, and Ala is substituted by Thr in the second box, as found in other teleost Aqp7 orthologs [32, 44].

Phylogenetic analyses of the previously cloned classical aquaporins [10] confirmed their identities as Aqp1aa and Aqp1ab and revealed that the newly cloned Aqp0 paralog is Aqp0a, while the partial Aqp4a sequence represents a duplicate of Aqp4 (Fig. 1A). Since this analysis represents the first evidence that teleost genomes retain more than one Aqp4 paralog, several transcripts and proteins were assembled de novo from whole-genome shotgun contigs available for Atlantic salmon (*Salmo salar*), Atlantic cod (*Gadus morhua*), and four cichlids: Zebra Mbuna (*Maylandia zebra*), Red mwanza (*Pundamilia nyererei*), Lyretail cichlid (*Neolamprologus brichardi*), and Burton's mouthbrooder (*Haplochromis burtoni*). Both the maximum likelihood and Bayesian analyses confirmed that the partial seabream Aqp4 sequence can be designated as Aqp4a, while the single zebrafish (*Danio rerio*) Aqp4 sequence previously isolated [32] is the Aqp4b ortholog. Phylogenetic analysis of the aquaglyceroporins confirmed the identity of the previously cloned seabream Aqp10b paralog [8] and revealed that the newly cloned sequences are Aqp3a, -7, and -9b, respectively (Fig. 1B).

Expression of Aquaporin Transcripts and Proteins in Seabream Testis and Sperm

The expression of aquaporin genes in the testis and ejaculated sperm was assessed by RT-PCR using paralog-specific primers designed from the previously and newly cloned cDNAs. The experiments indicated that *aqp0a*, *-1aa*, *-7*, *-8b*, *-9b*, and *-10b* were positively expressed in testis, whereas in sperm only *aqp1aa* and *-10b* transcripts were detected (Supplemental Fig. S1B). Interestingly, in contrast to our previous studies [10, 39], we also found low but detectable testicular expression levels of *aqp1ab* in the gilthead seabream. In contrast, neither *aqp3a* or *-4a* transcripts were detected in the testis or sperm, even with low stringency conditions for the PCR (i.e., reduced annealing temperature and/or increased cycle number; Supplemental Fig. S1B).

To investigate whether aquaporin mRNA expression in sperm and gonads correlated with that of the corresponding proteins, we produced affinity-purified antibodies for gilthead seabream Aqp0a, -7, -8b, and -9b. The specificity of these antibodies for the corresponding paralog, as well as of the antibodies against Aqp1aa, -1ab, and -10b previously produced, was tested by Western blot analysis of total membrane preparation from *X. laevis* oocytes expressing the different aquaporins (Supplemental Fig. S2). This analysis indicated that each antibody only recognized its target paralog, with no apparent cross-reaction with any of the other aquaporin polypeptides.

Western blots on protein extracts from testes using these antibodies showed reactive bands for Aqp0a, -1aa, -1ab, -7, -8b, -9b, and -10b of approximately the same molecular mass as the predicted monomers (28.7, 27.1, 28.2, 32.6, 27.9, 31.0, and 31.6 kDa, respectively; Fig. 2, A–G, arrowheads), thus supporting the RT-PCR data. Expression of the previously reported Aqp1aa and -10b paralogs in the ejaculated sperm

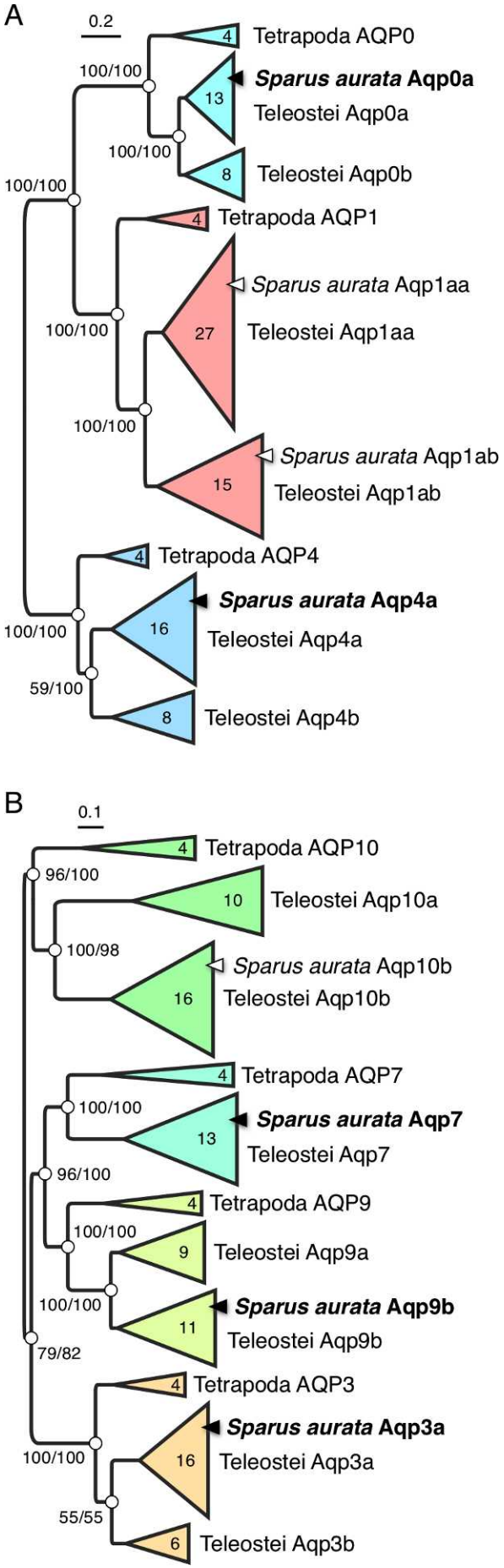

extracts [7] was confirmed here (Fig. 2, B and G), while the new findings show that Aqp1ab, -7, and -8b were also clearly detected (Fig. 2, C–E). These immunological results were consistent despite the fact that the corresponding transcripts could not be amplified from sperm total mRNA. In contrast, Aqp0a and -9b polypeptides were not detected in sperm (Fig. 2, A and F).

The Aqp1aa, -1ab, and -10b immunoblots showed additional reactive bands of higher molecular mass than the corresponding monomers, both in the testis and sperm protein extracts, which ranged from 45 to 60 kDa, 45 to 80 kDa, and 40 to 55 kDa, respectively (Fig. 2, B, C, and G). The specificity of these reactions was confirmed by the preincubation of the antisera with the corresponding immunizing peptides (Fig. 2, B, C, and G). Although these high-molecular-mass bands may correspond to aquaporin oligomers in sperm that are stable under reducing conditions, we tested whether they could also contain phosphorylated or N-linked glycosylated aquaporin forms by treating the protein extracts with CIP or PNGase F, respectively. After treatment with CIP, the 60-kDa sperm band detected with the Aqp1aa antibody was strongly reduced (Fig. 2B), suggesting that this band likely corresponds to a phosphorylated form. Moreover, a faint band of ~35 kDa appeared after PNGase F treatment (Fig. 2B), indicating that upper bands also include partially N-glycosylated Aqp1aa forms. For the sperm Aqp1ab, CIP treatment clearly reduced the 31-kDa band, as found for *X. laevis* oocytes expressing seabream Aqp1ab [10], but also induced the de novo detection of a ~28-kDa band (Fig. 2C). A band of a similar molecular mass also appeared after PNGase F treatment, suggesting that Aqp1ab and Aqp1aa are both phosphorylated and glycosylated in seabream sperm (Fig. 2, B and C). Aqp10b in sperm was detected as a major reactive band of ~31 kDa and various 40- to 55-kDa immunoreactive bands (Fig. 2G). The 55-kDa band disappeared with CIP treatment, and all of the 40- to 55-kDa bands were lowered with PNGase F treatment, while a de novo 33-kDa band appeared, suggesting that sperm Aqp10b may be highly phosphorylated and glycosylated (Fig. 2G).

Functional Characterization of Seabream Aquaporins

Previous studies using the *X. laevis* oocyte-swelling and radioactive uptake assays have determined that gilthead seabream Aqp1aa and −1ab are water-selective [9, 39], whereas Aqp10b is permeable to water, glycerol, and urea [7, 8]. The same experimental approaches were used to determine the permeation preferences of seabream Aqp0a, -7, -8b, and -9b (Fig. 3). Oocytes were injected with water as control or the aquaporin cRNA and exposed to hyposmotic shock, and the P_f was determined volumetrically. All aquaporins were efficiently translated and functional in oocytes, as their expression induced a significant 8- to 11-fold increase in the oocyte P_f, with water transport being significantly inhibited in the

FIG. 1. Summarized maximum likelihood tree of the codon alignments of orthologous vertebrate classical aquaporins (**A**) and aquaglyceroporins (**B**). The classical aquaporin tree is rooted with Inshore hagfish *aqp4*, while the aqualyceroporin tree is midpoint rooted. The seabream sequences cloned in the present study are indicated by black triangles, while the previously cloned seabream sequences are indicated with white triangles. Numbers within the summarized clusters represent the number of taxa analyzed. Statistical values at each node represent Bayesian posterior probabilities resulting from 5 million MCMC generations of full-length codon/amino acid alignments. Scale bars represent the rate of nucleotide substitution per site. A full list of taxa and accession numbers used in the study is provided in Supplemental Table S1.

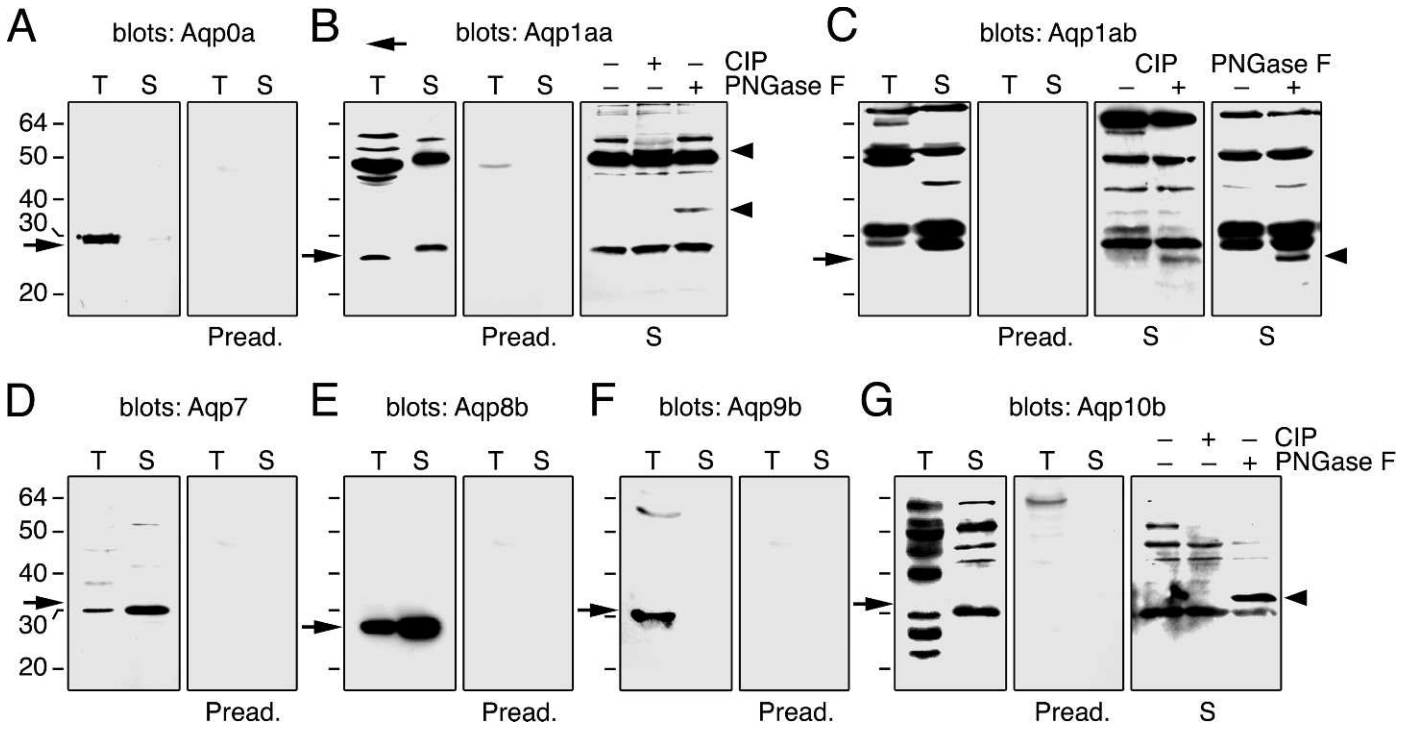

FIG. 2. Western blot analysis of aquaporins in gilthead seabream testis and spermatozoa. Approximately the same amount of protein (60 μg) of total testis (T) and sperm (S) was loaded in each lane, and membranes were probed with the different seabream aquaporin-specific antibodies as indicated in the top of each panel (**A**–**G**). Duplicated blots were run in parallel where immuno-incubation was performed using primary antibodies that had been preadsorbed (Pread.) by the antigenic peptides to test for specificity. For Aqp1aa, -1ab, and -10b, additional protein extracts from sperm were also digested with CIP or PNGase F prior to electrophoresis as indicated with plus or minus. Arrows indicate the target bands of the expected sizes based on in silico determination of molecular masses. The arrowheads point to CIP and/or PNGase F products. Molecular mass markers (kDa) are on the left.

presence of 0.1 mM $HgCl_2$ (Fig. 3A). However, while the P_f of oocytes expressing Aqp0a and -7 was only partially blocked by mercury, Aqp8b and -9b oocytes appear to be more sensitive to mercurial inhibition, since in these oocytes, 0.1 mM $HgCl_2$ reduced the P_f to near control levels. The mercurial inhibition of the P_f of Aqp0a- and -7-expressing oocytes was partially reversed by exposure to the reducing agent β-mercaptoethanol, but as previously observed for oocytes expressing seabream Aqp10b [7, 8], the inhibition of Aqp8b and -9b could not be recovered (Fig. 3A).

Isotope-labeled urea- and glycerol-uptake assays under isotonic conditions showed that oocytes injected with the water-specific Aqp0a were not permeable to either glycerol or urea (Fig. 3B). In contrast, oocytes expressing the aquaglyceroporins Aqp7 and -9b were permeable to both solutes, although in both cases urea permeability was somewhat lower (~6-fold with respect to controls) than that of glycerol (~8- to 9-fold with respect controls; Fig. 3B). Interestingly, oocytes expressing Aqp8b were also highly permeable to urea (~8-fold higher than controls), but this channel did not transport glycerol (Fig. 3B).

Cellular Localization of Aquaporins in the Seabream Testis and Efferent Duct

The cellular localization of the seven aquaporins in the seabream testis was determined by immunofluorescence microscopy using the affinity-purified antibodies (Figs. 4 and 5). The histological sections used for these studies were from testes of animals close to the spermiating period, and thus all stages of spermatogenic cells could be observed within the seminiferous tubules (Fig. 4, A–C). Some cysts contained mostly spermatogonia and type I and II spermatocytes (Fig. 4B), while most of the germ cells in other cysts were differentiated into spermatids and/or spermatozoa (Fig. 4C). Each cyst was delimited by the Sertoli cells, which in some cases had a flattened nucleus (Fig. 4, B and C). Aqp0a was the only aquaporin paralog observed in Sertoli cells, being strongly detected in the basal membrane and also in the cytoplasmic digitations enclosing the germ cells (Fig. 4, D and D'). Immunoreaction for Aqp1aa was specifically found in haploid germ cells, first appearing in the plasma membrane of spermatids and later found in the flagellum of spermatozoa released into the seminiferous tubule (Fig. 4, F and F'). In contrast, Aqp1ab was detectable in all germ cells from spermatogonia up to spermatozoa (Fig. 4, H and H'). The strong Aqp1ab staining in spermatogonia appeared predominantly intracellular, possibly in vesicles, whereas in spermatocytes and spermatids, the labeling became more concentrated in the plasma membrane. Spermatozoa inside the tubule did not show strong Aqp1ab staining, whereas a close examination of the sperm cells within the efferent duct revealed that Aqp1ab was present both in the head and the anterior region of the flagellum (Fig. 4H', inset).

As noted for Aqp1ab, Aqp7 immunoreaction was found in all germ cells (Fig. 5, A and A'). However, while the Aqp7 signals were the strongest in spermatogonia and spermatocytes, both in the cytoplasm and the plasma membrane, the signals decreased in spermatids and were detected only in the head of tubular spermatozoa (Fig. 5A', inset). Aqp8b polypeptides were first observed in the plasma membrane of spermatids and further strongly detected as a dotted-like pattern surrounding the nucleus of spermatozoa (Fig. 5, C and C'). The immunoreaction for Aqp9b was restricted to the plasma membrane and cytoplasm of isolated or grouped interstitial

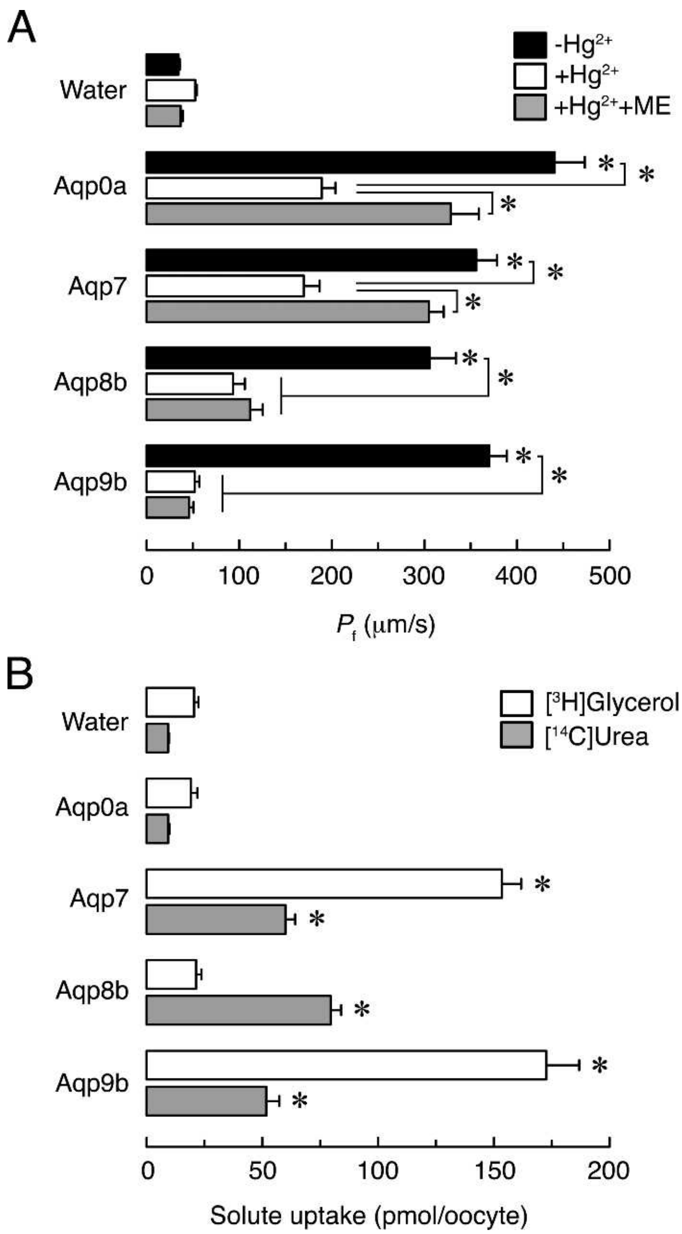

FIG. 3. Functional characterization of gilthead seabream aquaporins in *X. laevis* oocytes. Osmotic water permeability (P_f; **A**) and glycerol and urea uptake (**B**) of *X. laevis* oocytes injected with water as control or expressing different seabream aquaporins. The P_f was assayed in the presence or absence of 0.1 mM $HgCl_2$, and further incubation with 5 mM β-mercaptoethanol (ME), before and during the swelling assays. In **A** and **B**, values (mean ± SEM; n = 10–15 oocytes) with an asterisk are significantly ($P < 0.01$) different from water-injected oocytes, or between indicated treatments, in a representative experiment.

cells, and based on their distribution and nucleus morphology, they were most likely Leydig cells (Fig. 5, E and E'). Finally, the expression pattern of Aqp10b in the testis was similar to that of Aqp1ab and -7, with a strong staining in the plasma membrane of spermatogonia, spermatocytes, and spermatids, and also in both the head and flagellum of spermatozoa (Fig. 5, G and H). The specificity of the staining for each aquaporin was demonstrated by preincubation of antibodies with the immunizing peptides, which completely abolished the immunoreactions in all cases (Fig. 4, E, G, and I, and Fig. 5, B, D, F, and H). Altogether, the immunolocalization experiments showed a complex pattern of aquaporin expression and localization in the seabream testis (Table 1), where water as well as solute transport seems to be required at the onset of spermatogenesis

The expression of aquaporins in the seabream efferent duct was subsequently examined by immunohistochemistry (Fig. 6). In seabream males close to the spermiating phase, the efferent duct is characterized by a multilayered and folded epithelium showing regions of flat cells with a large vacuolated cytoplasm (Fig. 6A), as well as other regions in which the apical folds of the epithelial cells extend into the lumen and make contact with spermatozoa (Fig. 6C). Surprisingly, the only aquaporin we found expressed in the efferent duct epithelia was Aqp10b, since the other antibodies tested did not result in specific immunoreactions. Aqp1aa was, however, extensively expressed in the endothelia of blood vessels of the efferent duct (data not shown). The aquaglyceroporin Aqp10b was detected in the apical plasma membrane of the flat epithelial cells (Fig. 6B) as well as in the fibrous digitations enclosing spermatozoa (Fig. 6C). In both cell types, the membrane surrounding some of the intracellular vacuoles appeared to show Aqp10b immunoreaction (Fig. 6, white arrowheads in B and D insets). Preadsorption of the antiserum with the peptide led to a complete absence of staining (Fig. 6, E and F).

Aquaporin Localization in Seabream Spermatozoa and Changes During Motility Activation

The apparent differential expression of Aqp1aa, -1ab, -7, -8b, and -10b in sperm cells was investigated in more detail by immunofluorescence microscopy in ejaculated nonactivated and seawater-activated spermatozoa (Fig. 7, A–O). As an estimation of potential changes in aquaporin localization during activation of sperm motility, the fluorescence intensity of the immunoreaction for each antisera was measured in the head, as well as in the anterior and posterior regions of the flagellum (Fig. 7, P–T). The experiments indicated that Aqp1aa was specifically present in the flagellum of spermatozoa being homogenously distributed along its entire length (Fig. 7, A and B). No changes in Aqp1aa fluorescence intensity could be observed before or after motility activation (Fig. 7P). In contrast, although apparently less abundant than Aqp1aa, Aqp1ab was detected both in the plasma membrane of the head as well as dispersed along the flagellum (Fig. 7D). Upon activation, the immunostaining in the head appeared more intense, whereas the midpiece (basal to the head) became strongly labeled (Fig. 7E). Fluorescence measurements confirmed that Aqp1ab intensity in the head increased significantly, whereas no changes were observed either in the anterior or posterior tail (Fig. 7Q). Aqp7 was specifically located in the head of nonactivated and activated spermatozoa as dots in the plasma membrane, and its intensity or localization did not appear to change upon motility activation (Fig. 7, G, H, and R). Aqp8b was observed as diffuse areas around the nucleus in the head, with additional signal intensity of the immunoreaction stronger in the anterior part of the flagellum compared to the posterior region, but with no apparent concentration in the plasma membrane (Fig. 7J). After activation, total Aqp8b presence in the head did not change, but the immunoreaction almost completely relocated into the midpiece, with significantly reduced signal in both the anterior and posterior tail regions (Fig. 7, K and S). Finally, Aqp10b was observed in the plasma membrane of the head, midpiece, and along the entire flagellum, with slightly more abundance in the anterior part (Fig. 7M). As noted for Aqp1ab, a strong increase in Aqp10b immunofluorescence was observed in the head upon motility

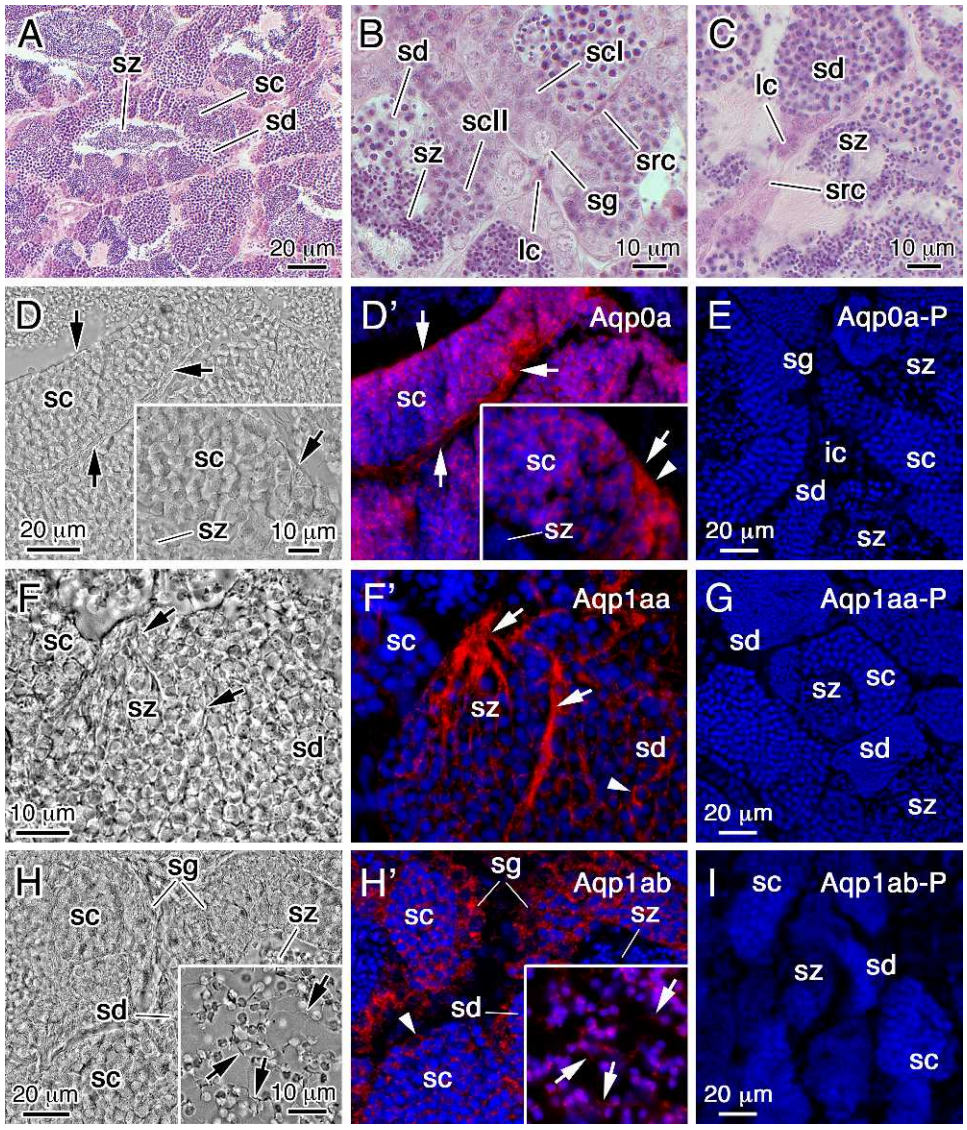

FIG. 4. Cellular localization of aquaporins in the gilthead seabream testis detected by immunofluorescence microscopy. **A–C**) Representative histological sections of testes stained with hematoxylin and eosin. Bright field (**D**, **F**, and **H**) and immunofluorescence (**D′**, **F′**, and **H′**) microscopy images of Aqp0a (**D** and **D′**), Aqp1aa (**F** and **F′**), and Aqp1ab (**H** and **H′**) localization. Sections were labeled with affinity-purified rabbit polyclonal antibodies. The reactions were visualized with Cy3-conjugated sheep IgG (red) and the nuclei were counterstained with DAPI (blue). Aqp0a expression was confined to Sertoli cells (arrows in **D′**), whereas Aqp1aa immunoreaction was found exclusively in spermatids and in the tail of spermatozoa (arrows in **F′**). Aqp1ab polypeptides were detected in all the germ cells, from spermatogonia to spermatids (**H′**). Spermatozoa inside the seminiferous tubule were negative for Aqp1ab (**H′**), but staining was detected in the head and tail of spermatozoa within the efferent duct (inset in **H′**). Arrowheads in **D′** (inset), **F′**, and **H′** point to the plasma membrane. **E**, **G**, **I**) Control sections incubated with preabsorbed antisera were negative. src, Sertoli cell; lc, Leydig cell; sg, spermatogonia; scI, spermatocyte type I; scII, spermatocyte type II; sd, spermatid; sz, spermatozoa.

activation in seawater, whereas the immunoreaction in the midpiece or the tail did not change (Fig. 7, N and T).

Since some of the aquaporins seemed to concentrate in the midpiece of the spermatozoa, approximately where the single mitochondrion of the seabream spermatozoon is confined [45], we next studied whether aquaporins may colocalize with the mitochondrion before or after activation. For these experiments, nonmotile and motile spermatozoa were preincubated with the mitochondrion-specific vital dye MitoTracker Red CMXRos prior to immunofluorescence microscopy. The results showed that Aqp1aa, -1ab, -7, and -10b were not found in the mitochondrion, either in NAM-diluted (data not shown) or in seawater-activated spermatozoa (Fig. 8, A–D). The same observation was noted for Aqp8b in nonmotile spermatozoa (Fig. 8E, left panel), but when motility was activated, Aqp8b seemed to translocate to the inner membrane of the mitochondrion (Fig. 8, E, right panel, and F).

Aquaporin Translocation to the Spermatozoa Plasma Membrane During Activation

The previous experiments suggested that some aquaporins are translocated into the spermatozoa plasma membrane during the activation of motility. Western blots of protein extracts from the plasma membrane of the head and flagella of spermatozoa were conducted to confirm the existence of this mechanism (Fig. 9). In these trials, the relative amount of each aquaporin in the plasma membrane was estimated from densitometric analyses of the reactive bands that corresponded to the monomers (including both phosphorylated and non-phosphorylated forms for Aqp1ab) in the plasma membrane

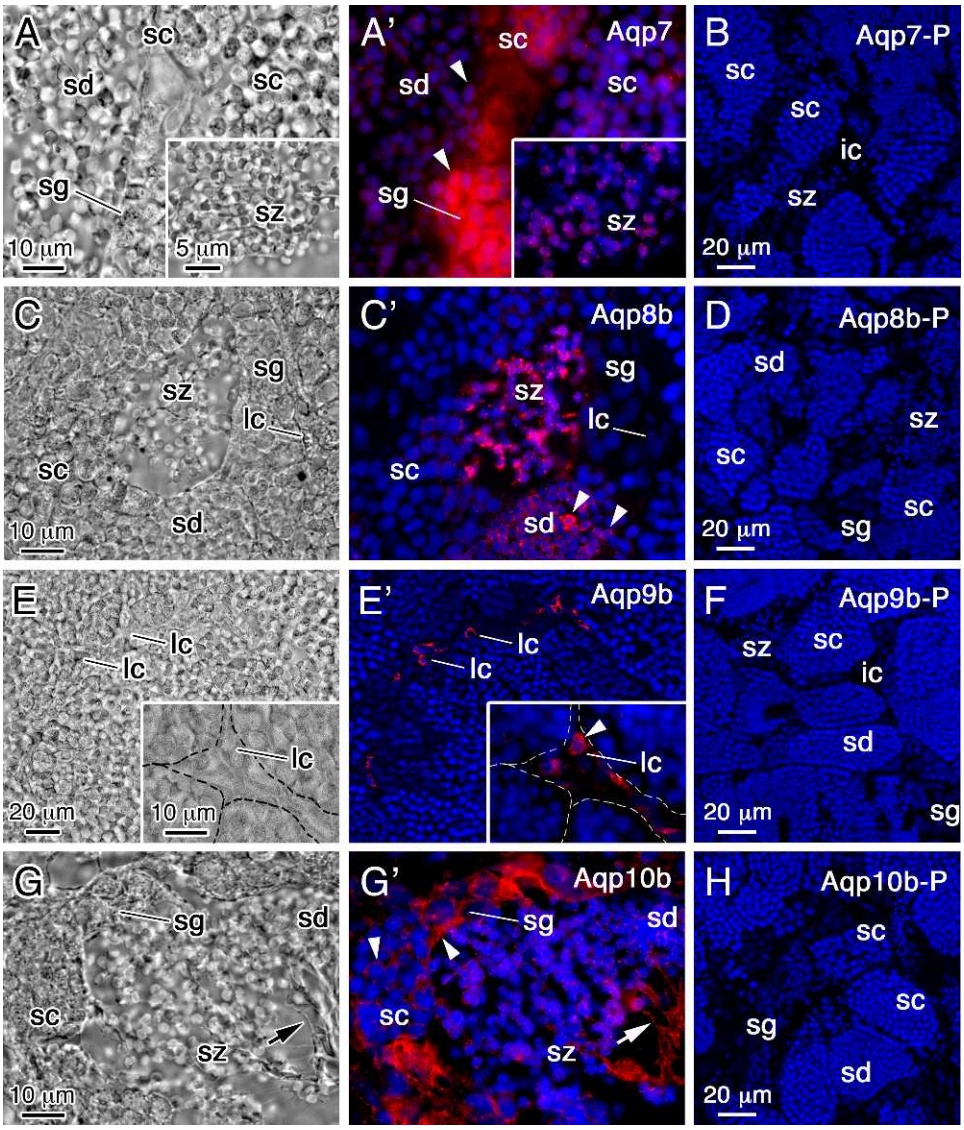

FIG. 5. Cellular localization of aquaporins in the gilthead seabream testis detected by immunofluorescence microscopy. Bright field (**A**, **C**, **E**, and **G**) and immunofluorescence (**A′**, **C′**, **E′**, and **G′**) microscopy images of Aqp7 (**A** and **A′**), Aqp8b (**C** and **C′**), Aqp9b (**E** and **E′**), and Aqp10b (**G** and **G′**) localization. Sections were labeled with affinity-purified rabbit polyclonal antibodies, except the anti-Aqp10b antiserum, and reactions were visualized as in Figure 4. Aqp7 and −10b immunoreactivities were found in all germ cells (**A′** and **G′**, respectively). In spermatozoa, Aqp7 staining was restricted to the head (**A′** inset), whereas that of Aqp10b was detected in the head and tail (arrows in **G′**). In contrast, Aqp8b polypeptides were detected only in spermatids and in the head of spermatozoa (**C′**), while Aqp9b immunoreactions were specific to Leydig cells surrounding the seminiferous tubules (**E′** and inset). Arrowheads in **A′**, **C′**, **E′** (inset), and **G′** point to the plasma membrane. **B**, **D**, **F**, and **H**) Control sections incubated with preabsorbed antisera were negative. Abbreviations as in Figure 4.

and total protein extracts (Fig. 9, A–D, right panels). As noted in the immunofluorescence microscopy experiments, the relative amount of Aqp1aa in the plasma membrane of the flagella was much higher than in the head, and it did not change after seawater activation (Fig. 9A). The same observation was made for Aqp7 in the head, where the relative amount in the plasma membrane remained unaffected by the hyperosmotic shock (Fig. 9C). The positive Aqp1aa reaction in the plasma membrane extract of the head, which was negative in previous immunocytochemical experiments, was possibly caused by the small contamination of the head preparation with short fragments of the anterior part of the flagella attached to the head, which were very difficult to separate (data not shown).

TABLE 1. Permeability properties and distribution of aquaporins in the gilthead seabream testis.

Aquaporin	Permeation preference	Cell type*
Aqp0a	Water	Src
Aqp1aa	Water	Sd, Sz
Aqp1ab	Water	Sg, Sc, Sd, Sz
Aqp7	Water, glycerol, and urea	Sg, Sc, Sd, Sz
Aqp8b	Water and urea	Sd, Sz
Aqp9b	Water, glycerol, and urea	Lc
Aqp10b	Water, glycerol, and urea	Sg, Sc, Sd, Sz

* Lc, Leydig cells; Src, Sertoli cells; Sg, spermatogonia; Sc, spermatocyte; Sd, spermatid; Sz, spermatozoa.

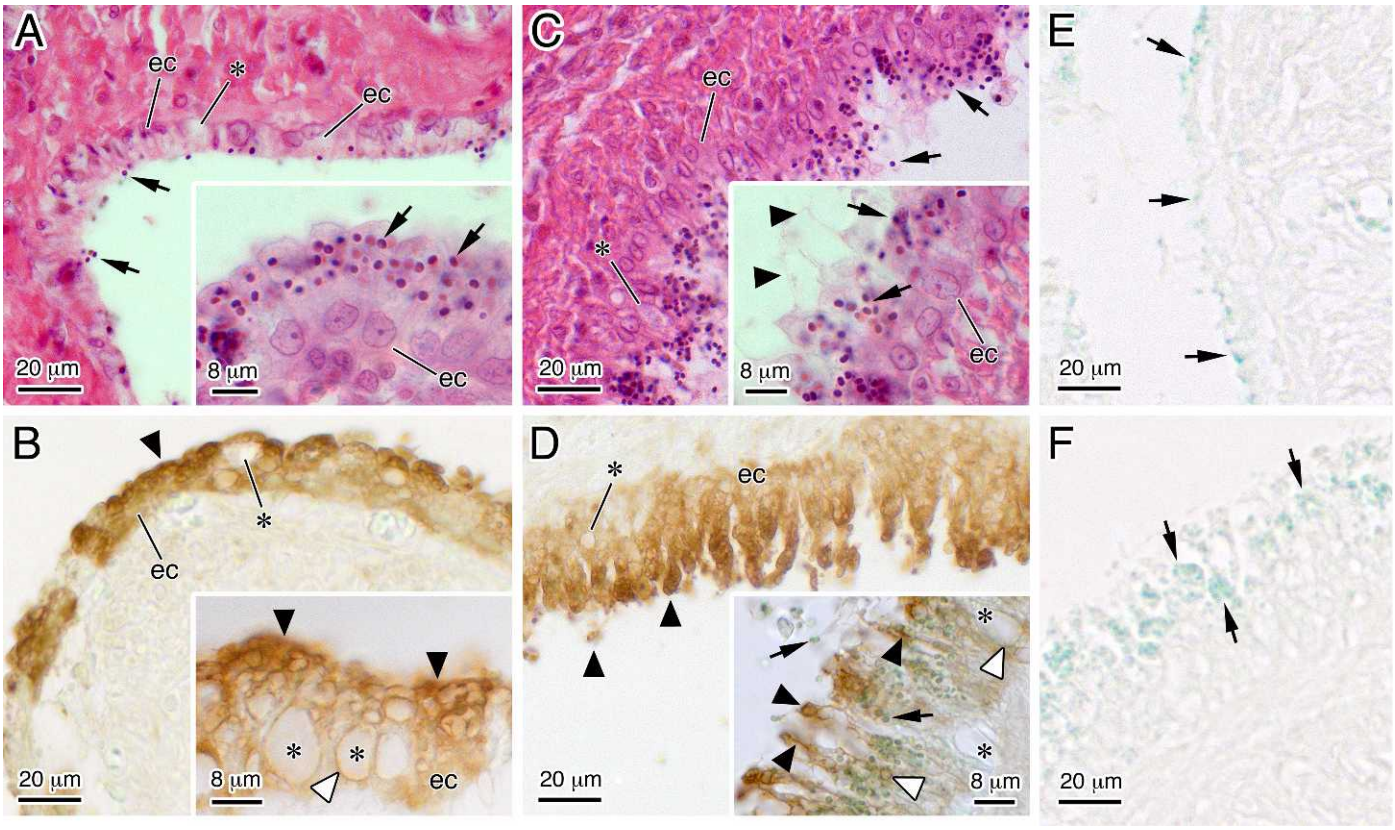

FIG. 6. Morphology of the testicular efferent duct of the gilthead seabream and immunohistochemical localization of Aqp10b. **A**, **C**) Histological sections of the columnar epithelial cells (ec) of the efferent duct including spermatozoa (arrows) stained with hematoxylin and eosin. The multilayered and folded duct epithelium shows regions with flat cells (**A** and inset) and other regions in which the apical folds of the epithelial cells extend into the lumen (**C**), indicative of a highly active epithelium. Note the vacuolated cytoplasm (asterisks) of the epithelial cells in both cases. **B**, **D**) Localization of Aqp10b in the duct epithelium. Sections were labeled with the anti-Aqp10b rabbit antiserum, and the presence of the antigen was visualized by the DAB method. Brownish peroxidase reaction product indicates the location of Aqp10b. The Aqp10b immunoreaction (arrowheads) was restricted to the apical membrane of flat and elongated epithelial cells (**B** and inset; **D** and inset). Aqp10b-positive signals were also noted apparently in the membrane of cytoplasmic vesicles (**B** and **D** insets, white arrowheads). **E** and **F**) Control sections incubated with preabsorbed antisera (arrows point to spermatozoa).

Unlike Aqp1aa and -7, seawater activation of spermatozoa seemed to control the translocation of Aqp1ab, -8b, and -10b into the plasma membrane. Thus, the relative amount of Aqp1ab in the plasma membrane of the head, but not in the flagella, was higher in activated compared to nonmotile spermatozoa (Fig. 9B). In addition, although Aqp1ab in the plasma membrane of spermatozoa seems to be partially phosphorylated both in the head and flagellum independently of activation, it appeared to be fully phosphorylated exclusively in the head upon the hyperosmotic shock. A similar scenario was observed for Aqp10b, which increased significantly in the plasma membrane of the head, but not in the flagella, during seawater activation (Fig. 9E). In the flagellum, the Aqp10b polypeptides in the plasma membrane seem to be more posttranslationally modified than in the head. In contrast to Aqp1ab and -10b, the Aqp8b channel in the head of spermatozoa appeared to be mostly intracellular, whereas in the flagellum this aquaporin was inserted in the plasma membrane, where its amount decreased in activated spermatozoa (Fig. 9D).

DISCUSSION

In the present study, we isolated five novel members of the aquaporin superfamily in gilthead seabream in order to investigate the potential role of multiple water channels in the testicular physiology of marine teleosts. Bayesian and maximum-likelihood analyses of the five novel members and the previously isolated aquaporin transcripts and encoded proteins [8, 32, 39] revealed that the seabream channels can be classified as either classical aquaporins, Aqp0a, -1aa, -1ab, and -4a, or as aquaglyceroporins, Aqp3a, -7, -9b, and -10b. To validate the phylogenetic classification, the permeability properties of the newly isolated channels were examined using ex vivo expression in *X. laevis* oocytes. Accordingly, these experiments confirmed that seabream Aqp0a is a water-selective channel, whereas Aqp3a (data not shown), -7, and -9b are permeable to water, glycerol, and urea. These data show that the seabream aquaporins have the same permeability preferences as the orthologs isolated from zebrafish [32] and mammals [20, 46, 47]. An interesting result was that seabream Aqp8b was highly permeable to urea in addition to water, but failed to transport glycerol. Mammalian aquaglyceroporins and AQP8 are known to be permeable to ammonia [48], but whether AQP8 also transports urea is controversial [49–51]. The high urea permeability of seabream Aqp8b is, however, not completely surprising, because zebrafish Aqp8aa, -8ab [32], and -8b (Chauvigné, Boj, and Cerdà, unpublished data), as well as the orthologs of Atlantic salmon [52], are all permeable to urea. In addition, some of the zebrafish (Chauvigné, Boj, and Cerdà, unpublished data) and Atlantic salmon [52] Aqp8 paralogs, such as Aqp8ab and -8b, can also transport glycerol, which is consistent with the fact that site-directed mutagenesis can convert a strictly water-permeable aquaporin into a channel permeable to ammonia alone or to

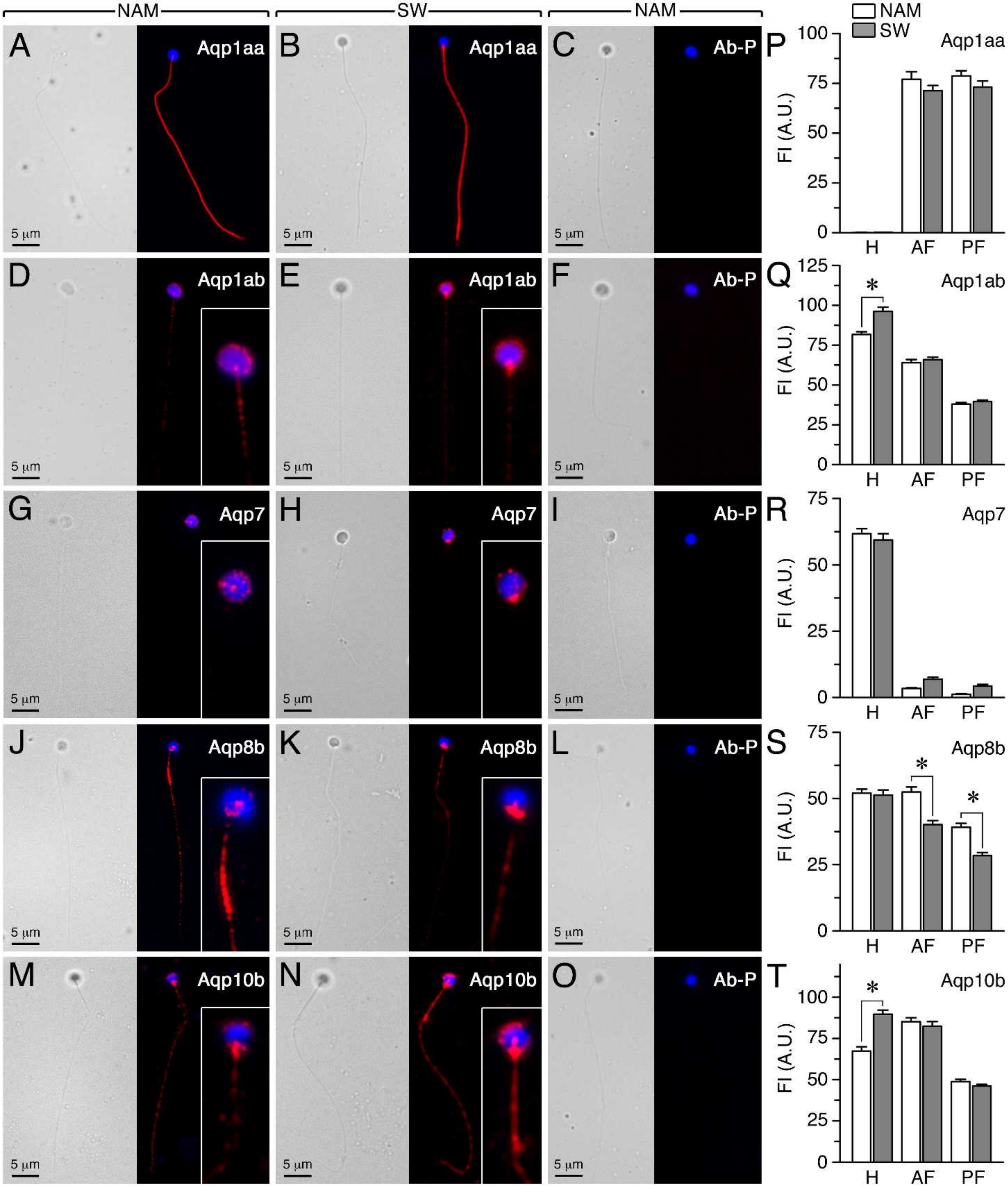

FIG. 7. Localization of aquaporins in ejaculated and seawater-activated spermatozoa of the gilthead seabream. Spermatozoa were diluted in NAM or activated in seawater (SW) for ~2 min and processed for immunofluorescence microscopy. Reactions were detected as in Figure 4. Representative bright field (**A–O**, left panels) and immunofluorescence (**A–O**, right panels) microscopy images of Aqp1aa (**A**, **B**), Aqp1ab (**D**, **E**), Aqp7 (**G**, **H**), Aqp8b (**J**, **K**), and Aqp10b (**M**, **N**) in NAM or SW-activated spermatozoa as indicated. In nonactivated spermatozoa, Aqp1aa and -7 immunoreactions were primarily localized to the tail and head, respectively, whereas those of Aqp1ab, -8b, and -10b appeared in both the tail and head. In SW-activated spermatozoa, Aqp1aa and -7 did not change significantly, whereas the Aqp1ab and -10b staining in the head was more prominent. In contrast, the Aqp8b immunoreaction in the tail decreased in SW, while the staining concentrated completely in the basal region of the head, presumably where the sperm mitochondria is localized. **C**, **F**, **I**, **L**, and **O**) Spermatozoa diluted in NAM probed with preadsorbed antibodies (Ab-P). **P–T**) Intensity of the immunofluorescence reactions (FI; arbitrary units) in the head (H), anterior flagellum (AF), and posterior flagellum (PF) for each antibody. Data are the mean ± SEM (n = 25–50 spermatozoa from four to five males). Values with an asterisk are significantly ($P < 0.05$) different between NAM- and SW-treated spermatozoa.

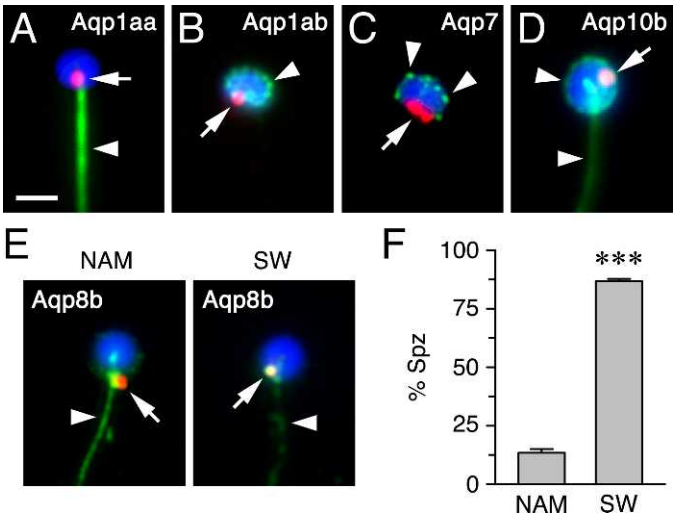

FIG. 8. Immunolocalization of aquaporins in mitochondria-labeled gilthead seabream spermatozoa. Sperm diluted in NAM and preincubated with the mitochondrion-specific vital dye MitoTraker Red CMXRos (red) were processed directly, or after activation in seawater (SW), for immunofluorescence microscopy (green). **A**, **B**) Neither Aqp1aa,-1ab, -7 nor -10b polypeptides (arrowheads) appeared to localize in the mitochondria (arrows) of activated (**A**, **B**, **C**, and **D**, respectively) or nonactivated (not shown) spermatozoa. **E**) In contrast, dilution of sperm with SW induced the colocalization of the MitoTraker (arrows) and Aqp8b (arrowheads) fluorescent signals (yellow) in the head, suggesting the translocation of Aqp8b into the mitochondria in motile sperm. **F**) Percentage of NAM and SW spermatozoa showing complete accumulation of Aqp8b in the mitochondria. Data are the mean ± SEM (n = 150 spermatozoa from six males). ***$P < 0.001$ versus NAM-treated spermatozoa.

ammonia, urea, and glycerol [48, 53]. However, the molecular basis for seabream Aqp8b discriminating between urea and glycerol permeation is yet unknown.

Expression of *aqp0a*, *-1aa*, *-7*, *-8b*, *-9b*, and *-10b* mRNAs were each detected in the gilthead seabream testis by RT-PCR, while the corresponding protein expression was demonstrated by Western blotting using affinity-purified, paralog-specific antibodies. The specificity of each antibody was confirmed by the disappearance of target bands after adsorption with excess antigen peptides. Immunoblotting, thus, revealed major bands for all aquaporins at the expected monomer size around 25–32 kDa, but also a number of reactive polypeptides of higher molecular mass for Aqp1aa, -1ab, and -10b but not for Aqp0a, -7, -8b, and -9b. Such high-molecular-mass bands have been previously observed for seabream Aqp1aa [7, 9] and for other species of fish, including Aqp1ab in Atlantic halibut (*Hippoglossus hippoglossus*) [34], Aqp1aa and -8ab in Atlantic salmon [54], Aqp11 in zebrafish [55], and Aqp4 in the spiny dogfish (*Squalus acanthias*) [56]. These high–molecular-mass bands appear to represent oligomers as well as variable glycosylated and phosphorylated forms of the proteins. The present results show that seabream Aqp1aa and -10b are expressed in the testis and confirm the earlier report of their expression in the ejaculated sperm of seabream [7]. In addition, we found that the seabream Aqp1ab, which is highly expressed in the oocyte and mediates oocyte hydration during meiotic maturation [34, 37, 39, 57], is also synthesized and extensively posttranslationally modified in the testis, as observed in the ovary [37, 57]. This new finding agrees with the detection of *aqp1ab* transcripts in the testis of the zebrafish [32], Japanese eel (*Anguilla japonica*) [58], and Atlantic halibut [34], but contrasts with data for the European eel (*Anguilla anguilla*) [10], Senegalese sole (*Solea senegalensis*) [10], Stinging catfish (*Heteropneustes fossilis*) [59], and half-smooth tongue sole (*Cynoglossus semilaevis)* [60], in which the testicular expression of *aqp1ab* has not been noted. These discrepancies may be related to the much lower level of *aqp1ab* expression in the testis compared to the ovary in species that produce highly or moderately hydrated eggs (e.g., gilthead seabream, European eel, or Stinging catfish), which may prevent the amplification of *aqp1ab* transcripts when the same PCR conditions are used for both tissues. The gilthead seabream thus expresses at least seven distinct aquaporin paralogs in the testis, which represents a slightly lower number than in the zebrafish, where expression of *aqp1aa*, *-1ab*, *-3a*, *-3b*, *-4*, *-7*, *-8aa*, *-10b*, and *-12* was reported [32]. Interestingly, the prevalence of *aqp7* and *aqp8*-like paralogs in the testis of both mammals and teleosts, as well as the expression of *aqp1aa*, *-1ab*, and *-10b* between evolutionary distant teleosts, indicates that their roles may be conserved. However, because the complete genomic repertoire of aquaporins in the gilthead seabream is not yet available, the exact number of aquaporin paralogs expressed in the seabream testis remains to be determined.

Immunofluorescence microscopy revealed that among the seven aquaporins investigated in the seabream testis, only Aqp0a and -9b are specifically localized in the Sertoli and Leydig cells, respectively. The presence of these orthologs in seabream Sertoli and Leydig cells is conserved with respect to mammals since this has been previously reported in rats (*Rattus norvegicus*) [12–14, 19, 61], although the expression of AQP9 was undetectable in the testis of the dog (*Canis lupus familiaris*), fruit-eating bat (*Artibeus lituratus*), mouse (*Mus musculus*), and human [47, 62–64]. Mammalian Sertoli and Leydig cells also express the AQP8 and -0 orthologs, respectively [12, 16, 65], and in avian species AQP5, which is not conserved in the zebrafish genome [32], is specifically found in Leydig cells [66]. Although Aqp8b protein expression could not be demonstrated in seabream Sertoli cells, it is still possible that other Aqp8 paralogs, such as Aqp8aa, which is phylogenetically closer to the tetrapod AQP8 than to Aqp8b [30], are present in these cells. Similarly, other seabream aquaporin paralogs, including Aqp0b, which is detected in the zebrafish testis at the mRNA level [32], may also be present in Leydig cells. In the seabream, the function of Aqp9b in the steroid-secreting Leydig cells is unknown, but in the Sertoli cells, it is possible that Aqp0a is involved in the process of hormone-induced hydration of the seminal fluid that occurs during the spermiating phase in teleosts [67]. In addition, a function of Aqp0a to maintain the barrier between the interstitial/blood compartment and the lumen of the seminiferous tubules may also be considered, since this aquaporin also plays a role in cell adhesion [68]. In rats, however, AQP0 is mainly expressed in Sertoli cells delimitating seminiferous tubules containing elongated spermatids [12], whereas in seabream, Aqp0a is detected in Sertoli cells of cysts containing all stages of the spermatogenic cells. Since we only studied testes at the spermiating phase in the present study, it is unknown whether seabream Aqp0a can be specifically upregulated in Sertoli cells at this stage.

The testicular pattern of germ cell growth from diploid spermatogonia to spermatocytes and haploid spermatids, and the subsequent differentiation into spermatozoa, are in general similar between teleosts and mammals [69, 70]. The present data for aquaporin expression in the seabream germ cells reveal that the pattern is reminiscent of that in mammals [21]. In the seabream, five different aquaporins, Aqp1aa, -1ab, -7, -8b, and -10b, are expressed in differentiating germ cells, which may highlight the importance of water and solute transport during

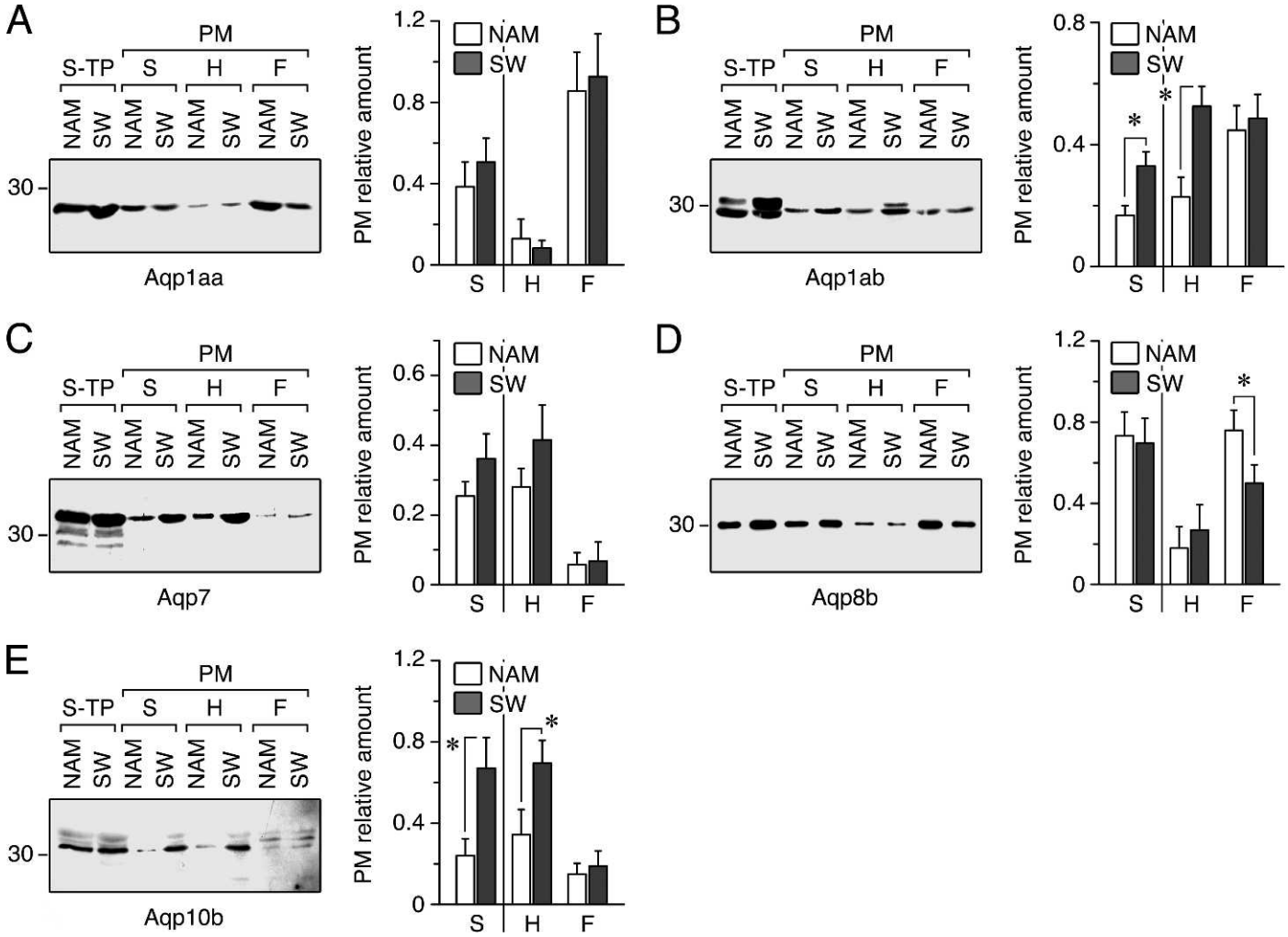

FIG. 9. Relative amount of aquaporin polypeptides in the plasma membrane of gilthead seabream spermatozoa before and after motility activation. **A–E**) Representative Western blots of sperm total protein extracts (S-TP; 60 μg) and plasma membrane extracts (PM; 40 μg) of intact sperm (S) and spermatozoa head (H) and flagellum (F) probed with the different aquaporin antibodies as indicated. Samples were taken from NAM and SW sperm. A 30-kDa molecular mass marker is shown on the left of each blot. On the right of each panel is the relative amount (mean ± SEM; n = 5 males) of each aquaporin monomer in the PM with respect to its amount in the total protein extract determined by densitometric analysis of the reactive bands. For Aqp1ab, both phosphorylated and nonphosphorylated forms were taken for the analysis. Values with an asterisk are significantly ($P < 0.05$) different between NAM- and SW-treated spermatozoa.

spermatogenesis. Their pattern of expression was, however, not completely redundant, because although Aqp1ab, -7 and -10b were detected in all germ cells, from spermatogonia to spermatozoa, Aqp1aa and -8b were first noted only in haploid spermatids and sperm. These findings suggest that Aqp1aa and -8b may be needed during the spermiogenic phase of strong cytoplasmic reduction and flagella formation, presumably caused by an intense water efflux [71]. In line with this notion is the observation that Aqp1aa is the only aquaporin found abundantly distributed along the entire flagella of ejaculated spermatozoa. Such a pattern of aquaporin expression in the male germ cells of seabream is similar to that described in tetrapods, since in these species AQP1 and -7 are localized in round and/or elongated spermatids [21, 23, 24, 64, 66]. However, in mammals, it is quite likely that species-specific differences in AQP8 localization in germ cells exist, including restriction to certain spermatogenic cell types or to all germ cells, or even exclusive expression in Sertoli cells [3]. In addition, AQP11, an ortholog that has not been investigated in the present study, is found in the caudal cytoplasm of elongating spermatids of rodents, where it might be involved in the release of the residual body [22].

Aquaporin expression in the seabream efferent duct was also investigated in the present study. In mammals, the efferent duct, together with the epididymis, are responsible for the reabsorption of seminal fluid and the release of nutritional factors that allow sperm concentration and cell survival [72]. Teleosts do not develop a proper epididymis but show spermatic ducts and testicular efferent ducts, which are also involved in the storage, nutrition, and resorption of spermatozoa [73]. In the mammalian efferent duct and epididymis, a broad expression of aquaporins is found, where AQP1, -3, -9, and -10 are detected in ciliated and nonciliated epithelial cells [12, 13, 18, 19]. In the efferent duct of spermiating seabream, we could only consistently detect Aqp10b polypeptides, which were localized in the plasma membrane of the luminal epithelial cells. As suggested for the rat epididymis [74], the expression of the glycerol-transporting Aqp10b paralog in the seabream efferent duct may mediate water transport and provide glycerol as an aerobic metabolic substrate for spermatozoa [75, 76].

Immunolocalization and Western blotting confirmed that the five aquaporins present in seabream intratubular spermatozoa, Aqp1aa, -1ab, -7, -8b, and -10b, persisted in the ejaculated sperm, even though *aqp1ab*, *-7*, and *-8b* mRNAs were not detectable. Such differences in positive detection between PCR and Western blotting have been observed previously in human ejaculated spermatozoa [21] and may be related to the degradation of the *aqp1ab*, *-7*, and *-8b* mRNAs after synthesis of the proteins in the testis. In any event, our immunofluorescence microscopy studies showed specific spatial distributions of the aquaporins in ejaculated spermatozoa of seabream, where Aqp1aa and -7 are restricted to the flagellum and head, respectively, whereas Aqp1ab, -8b, and -10b are present in both regions, although in the flagellum they appeared to be more accumulated in the anterior region. In addition, the Western blot analyses indicated that in nonactivated spermatozoa the amount of Aqp1ab and -10b in the plasma membrane seems to be lower than that of Aqp1aa, -7, or -8b. The spermatozoa of mammals also express the AQP7 and -8 orthologs, but their localization differs from that in the seabream, since AQP7 is localized in the cytoplasmic droplet and/or the middle piece of the tail and AQP8 is present as a punctuated pattern in the cytoplasmic droplet and along the tail [21, 24, 26, 77]. The expression of Aqp10b in the head and flagella of seabream spermatozoa agrees with our previous report [7], but this is not the case for Aqp1aa, which was previously detected in the head and tail. In the present study we found the Aqp1aa protein exclusively localized along the entire flagellum. This inconsistency is most likely caused by the immunohistochemical protocol employed, since in the previous study we used peroxidase staining, whereas the present work employed immunofluorescence, which is more sensitive and allowed us to use a 100-fold higher dilution of the same primary antibody with respect to the previous report. In addition, in the present study, preincubation of the antiserum with the antigenic peptide completely removed positive immunofluorescence signals in the flagellum. These data strongly suggest that seabream Aqp1aa is present only in the flagellum of spermatozoa, which differs from mammals, where the expression of AQP1 in spermatozoa has not been consistently demonstrated except for canine spermatozoa, although there was no report on the localization of the protein [78]. In mice and humans, AQP11 is localized at the end piece of the sperm flagellum just prior to spermiation [22], and AQP3 is in the principal piece of the sperm tail, where it is possibly involved in sperm volume regulation during oviductal migration [28]. In the seabream, we could not confirm *aqp3a* expression at the mRNA level in the testis or sperm, but whether the Aqp3b protein is present in seabream spermatozoa needs to be conclusively determined using specific antibodies.

The spatial segregation of aquaporins in the ejaculated sperm of seabream is consistent with the hypothesis that these channels may play different roles during the seawater activation or maintenance of sperm motility in marine teleosts [1, 7, 11, 79–81]. In our previous work, we confirmed that both Aqp1aa and -10b were present in seabream spermatozoa and concluded that Aqp1aa possibly mediates the water efflux during the hyperosmotic shock required for sperm activation, whereas Aqp10b may be involved in the maintenance of motility [7]. This conclusion was based on the observation that mercury inhibited Aqp1aa- and -10b-mediated water transport in *X. laevis* oocytes [7–9], as well as sperm activation and the associated phosphorylation and dephosphorylation events [7, 29]. Both effects can be recovered with β-mercaptoethanol, to which $HgCl_2$-inhibited Aqp10b is not sensitive [7, 8]. In the present study, however, we demonstrated that seabream spermatozoa express not only Aqp1aa and -10b but also Aqp1ab, -7, and -8b. In addition, immunofluorescence microscopy and Western blotting of purified plasma membranes of head- and tail-enriched fractions indicate that Aqp1aa and -7 localization do not change during activation of spermatozoa motility in seawater, whereas the amount of Aqp1ab and -10b in the head plasma membrane is significantly increased. These findings show that rather than Aqp1aa and -10b being translocated to the plasma membrane, as suggested by Zilli et al. [7], it is the Aqp1ab and -10b channels that are inserted into the plasma membrane during spermatozoan activation. This observation, together with the fact that mercurial inhibition of seabream Aqp1ab and -7 can be reversed by β-mercaptoethanol as in Aqp1aa [10, 39] and that phosphorylated Aqp1ab accumulates in the plasma membrane upon activation, uncovers a role of Aqp1ab rather than of Aqp1aa in the hyperosmotic activation of sperm motility in seabream. However, because Aqp1aa polypeptides are distributed along the entire flagellum of both nonmotile and motile spermatozoa, it is still plausible that Aqp1aa plays an important role in activating or maintaining the flagella movement. Interestingly, the phosphorylated form of Aqp1ab is retained in the cytoplasm when ectopically expressed in *X. laevis* oocytes, which is contrary to what seems to be the case in seabream spermatozoa [10]. Future studies will, therefore, be required to elucidate the specific contribution of Aqp1aa and -1ab in the mechanism of initiation and maintenance of sperm motility in the gilthead seabream, as well as their trafficking regulation.

The occurrence of AQP7 and -8 orthologs in seabream spermatozoa, as well as in the testis, is conserved with respect to mammals, suggesting that these channels may be essential for sperm physiology in vertebrates. However, the roles of testicular AQP7 and -8 in tetrapods remain intriguing because knockout mice models show normal spermatogenesis, sperm morphology, and kinematic characteristics [82, 83], although AQP8 may be a candidate for the control of volume regulation of murine spermatozoa [27]. In seabream, there is redundant expression of two aquaglyceroporins in ejaculated sperm, Aqp7 and -10b, which are differentially regulated during sperm activation. The physiological significance of this dual expression is unknown, although the presence of Aqp7 might be reminiscent of its role in glycerol utilization in energy metabolism in sperm of the seminiferous tubules or in the efferent duct. Nevertheless, in this study we found that during seawater activation, seabream Aqp8b is relocated from the plasma membrane of the anterior flagellum into the mitochondrion of spermatozoa, which did not occur for the other aquaporins. Although such a mechanism for AQP8 has not been previously observed in mammalian sperm, the accumulation of AQP7 in the mitochondria of human activated spermatozoa [26], as well as the presence of AQP8 in the inner membrane of the mitochondria of several tissues [84–87], has been reported. Since AQP7 and -8 are permeable to ammonia in addition to water and solutes [48, 88], and AQP8 does not appear to contribute greatly to the facilitated transport of water across the mitochondrial membrane [82, 89, 90], it is plausible that the major function of mitochondrial AQP8 is ammonia diffusional transport [90]. In the liver and renal proximal tubule cells, AQP8 may be involved in mitochondrial ammonia detoxification during amino acid metabolism via ureagenesis (urea cycle) [90] or by facilitating ammonia excretion by the apical Na^+/H^+ exchanger NHE3, thus restoring the acid-base balance [87]. However, because AQP8 is also permeable to hydrogen peroxide (H_2O_2), the potential relevance of mitochondrial AQP8 in the generation of reactive oxygen species

(ROS) can also be considered [91, 92]. Teleost Aqp8 orthologs are potentially permeable to ammonia and H_2O_2, since they show the structural features common to mammalian AQP8, which allow these molecules to pass [30]. Therefore, in spite of its high urea conductance, it is possible that Aqp8b in the mitochondria of activated seabream sperm is involved in the release from the mitochondrial matrix of H_2O_2 and ammonia, which are generated from oxidative phosphorylation and amino acid metabolism occurring during the swimming phase of marine fish spermatozoa [93]. This mechanism would help to prevent the deleterious consequences of hyperammonemia in swimming spermatozoa, as well as ROS-induced mitochondrial dysfunction and subsequent cell death [90, 94]. The ability of teleost Aqp8 orthologs to permeate ammonia or H_2O_2 has, however, not yet been demonstrated and, therefore, this hypothesis should be investigated.

In conclusion, by using both immunohistochemical and biochemical approaches, we established for the first time the presence of up to seven different aquaporin paralogs in the male reproductive tract of a nonmammalian vertebrate. The data show that the expression pattern and localization of several aquaporins in the testis as well as in ejaculated and activated spermatozoa is strikingly similar to that described in mammals. Our findings strongly suggest that aquaporins may play different but overlapping roles during spermatogenesis and spermiogenesis in marine teleosts, with selected paralogs being rapidly redistributed to the spermatozoan plasma membrane for the initiation and maintenance of sperm motility.

REFERENCES

1. Cosson J. The ionic and osmotic factors controlling motility of fish spermatozoa. Aqua Int 2004; 12:69–85.
2. Huang HF, He RH, Sun CC, Zhang Y, Meng QX, Ma YY. Function of aquaporins in female and male reproductive systems. Hum Reprod Update 2006; 12:785–795.
3. Yeung CH. Aquaporins in spermatozoa and testicular germ cells: identification and potential role. Asian J Androl 2010; 12:490–499.
4. Finn RN, Kristoffersen BA. Vertebrate vitellogenin gene duplication in relation to the ''3R hypothesis'': correlation to the pelagic egg and the oceanic radiation of teleosts. PLoS ONE 2007; 2:e169.
5. Cerdà J, Zapater C, Chauvigné F, Finn RN. Water homeostasis in the fish oocyte: new insights into the role and molecular regulation of a teleost-specific aquaporin. Fish Physiol Biochem 2013; 39:19–27.
6. Zilli L, Schiavone R, Storelli C, Vilella S. Molecular mechanisms determining sperm motility initiation in two sparids (*Sparus aurata* and *Lithognathus mormyrus*). Biol Reprod 2008; 79:356–366.
7. Zilli L, Schiavone R, Chauvigné F, Cerdà J, Storelli C, Vilella S. Evidence for the involvement of aquaporins in sperm motility activation of the teleost gilthead sea bream (*Sparus aurata*). Biol Reprod 2009; 81: 880–888.
8. Santos CR, Estêvão MD, Fuentes J, Cardoso JC, Fabra M, Passos AL, Detmers FJ, Deen PM, Cerdà J, Power DM. Isolation of a novel aquaglyceroporin from a marine teleost (*Sparus auratus*): function and tissue distribution. J Exp Biol 2004; 207:1217–1227.
9. Raldúa D, Otero D, Fabra M, Cerdà J. Differential localization and regulation of two aquaporin-1 homologs in the intestinal epithelia of the marine teleost *Sparus aurata*. Am J Physiol Regul Integr Comp Physiol 2008; 294:R993–R1003.
10. Tingaud-Sequeira A, Chauvigné F, Fabra M, Lozano J, Raldúa D, Cerdà J. Structural and functional divergence of two fish aquaporin-1 water channels following teleost-specific gene duplication. BMC Evol Biol 2008; 8:259.
11. Cosson J, Dreanno C, Fauvel C, Groison AL, Suquet M, Billard R. Marine fish spermatozoa: racing ephemeral swimmers. Reproduction 2008; 136: 277–294.
12. Hermo L, Krzeczunowicz D, Ruz R. Cell specificity of aquaporins 0, 3, and 10 expressed in the testis, efferent ducts, and epididymis of adult rats. J Androl 2004; 25:494–505.
13. Badran HH, Hermo LS. Expression and regulation of aquaporins 1, 8, and 9 in the testis, efferent ducts, and epididymis of adult rats and during postnatal development. J Androl 2002; 23:358–373.
14. Nihei K, Koyama Y, Tani T, Yaoita E, Ohshiro K, Adhikary LP, Kurosaki I, Shirai Y, Hatakeyama K, Yamamoto T. Immunolocalization of aquaporin-9 in rat hepatocytes and Leydig cells. Arch Histol Cytol 2001; 64:81–88.
15. Nagano T, Suzuki F. Cell junctions in the seminiferous tubule and the excurrent duct of the testis. Int Rev Cytol 1983; 81:163–190.
16. Calamita G, Mazzone A, Bizzoca A, Svelto M. Possible involvement of aquaporin-7 and -8 in rat testis development and spermatogenesis. Biochem Biophys Res Commun 2001; 288:619–625.
17. Rato L, Socorro S, Cavaco JE, Oliveira PF. Tubular fluid secretion in the seminiferous epithelium: ion transporters and aquaporins in Sertoli cells. J Membr Biol 2010; 236:215–224.
18. Oliveira CA, Carnes K, França LR, Hermo L, Hess RA. Aquaporin-1 and -9 are differentially regulated by oestrogen in the efferent ductule epithelium and initial segment of the epididymis. Biol Cell 2005; 97: 385–395.
19. Elkjaer M, Vajda Z, Nejsum LN, Kwon T, Jensen UB, Amiry-Moghaddam M, Frøkiaer J, Nielsen S. Immunolocalization of AQP9 in liver, epididymis, testis, spleen, and brain. Biochem Biophys Res Commun 2000; 276:1118–1128.
20. Ishibashi K, Kuwahara M, Gu Y, Kageyama Y, Tohsaka A, Suzuki F, Marumo F, Sasaki S. Cloning and functional expression of a new water channel abundantly expressed in the testis permeable to water, glycerol, and urea. J Biol Chem 1997; 272:20782–20786.
21. Yeung CH, Callies C, Tüttelmann F, Kliesch S, Cooper TG. Aquaporins in the human testis and spermatozoa—identification, involvement in sperm volume regulation and clinical relevance. Int J Androl 2010; 33:629–641.
22. Yeung CH, Cooper TG. Aquaporin AQP11 in the testis: molecular identity and association with the processing of residual cytoplasm of elongated spermatids. Reproduction 2010; 139:209–216.
23. Calamita G, Mazzone A, Cho YS, Valenti G, Svelto M. Expression and localization of the aquaporin-8 water channel in rat testis. Biol Reprod 2001; 64:1660–1666.
24. Saito K, Kageyama Y, Okada Y, Kawakami S, Kihara K, Ishibashi K, Sasaki S. Localization of aquaporin-7 in human testis and ejaculated sperm: possible involvement in maintenance of sperm quality. J Urol 2004; 172:2073–2076.
25. Morishita Y, Matsuzaki T, Hara-chikuma M, Andoo A, Shimono M, Matsuki A, Kobayashi K, Ikeda M, Yamamoto T, Verkman A, Kusano E, Ookawara S, et al. Disruption of aquaporin-11 produces polycystic kidneys following vacuolization of the proximal tubule. Mol Cell Biol 2005; 25:7770–7779.
26. Moretti E, Terzuoli G, Mazzi L, Iacoponi F, Collodel G. Immunolocalization of aquaporin 7 in human sperm and its relationship with semen parameters. Syst Biol Reprod Med 2012; 58:129–135.
27. Yeung CH, Callies C, Rojek A, Nielsen S, Cooper TG. Aquaporin isoforms involved in physiological volume regulation of murine spermatozoa. Biol Reprod 2009; 80:350–357.
28. Chen Q, Peng H, Lei L, Zhang Y, Kuang H, Cao Y, Shi QX, Ma T, Duan E. Aquaporin3 is a sperm water channel essential for postcopulatory sperm osmoadaptation and migration. Cell Res 2011; 21:922–933.
29. Zilli L, Beirão J, Schiavone R, Herraez MP, Cabrita E, Storelli C, Vilella S. Aquaporin inhibition changes protein phosphorylation pattern following sperm motility activation in fish. Theriogenology 2011; 76:737–744.
30. Cerdà J, Finn RN. Piscine aquaporins: an overview of recent advances. J Exp Zool A Ecol Genet Physiol 2010; 313:623–650.
31. Chauvigné F, Zapater C, Cerdà J. Role of aquaporins during teleost gametogenesis and early embryogenesis. Front Physiol 2011; 2:66.
32. Tingaud-Sequeira A, Calusinska M, Finn RN, Chauvigné F, Lozano J, Cerdà J. The zebrafish genome encodes the largest vertebrate repertoire of functional aquaporins with dual paralogy and substrate specificities similar to mammals. BMC Evol Biol 2010; 10:38.
33. Finn RN, Cerdà J. Aquaporin evolution in fishes. Front Physiol 2011; 2: 44.
34. Zapater C, Chauvigné F, Norberg B, Finn RN, Cerdà J. Dual neofunctionalization of a rapidly evolving aquaporin-1 paralog resulted in constrained and relaxed traits controlling channel function during meiosis resumption in teleosts. Mol Biol Evol 2011; 28:3151–3169.
35. Katoh K, Toh H. Recent developments in the MAFFT multiple sequence alignment program. Brief Bioinform 2008; 9:286–298.
36. Suyama M, Torrents D, Bork P. PAL2NAL: robust conversion of protein sequence alignments into the corresponding codon alignments. Nucleic Acids Res 2006; 34:W609–W612.
37. Fabra M, Raldúa D, Bozzo MG, Deen PMT, Lubzens E, Cerdà J. Yolk proteolysis and aquaporin-1o play essential roles to regulate fish oocyte hydration during meiosis resumption. Dev Biol 2006; 295:250–262.
38. Zampighi GA, Kreman M, Boorer KJ, Loo DDF, Bezanilla F, Chandy G,

Hall JE, Wright EM. A method for determining the unitary functional capacity of cloned channels and transporters expressed in *Xenopus laevis* oocytes. J Membr Biol 1995; 148:65–78.
39. Fabra M, Raldúa D, Power DM, Deen PM, Cerdà J. Marine fish egg hydration is aquaporin-mediated. Science 2005; 307:545.
40. de Curtis I, Fumagalli G, Borgese N. Purification and characterization of two plasma membrane domains from ejaculated bull spermatozoa. J Cell Biol 1986; 102:1813–1825.
41. Labbé C, Loir M. Plasma membrane of trout spermatozoa: I. Isolation and partial characterization. Fish Physiol Biochem 1991; 9:325–338.
42. Beirão J, Zilli L, Vilella S, Cabrita E, Schiavone R, Herráez MP. Improving sperm cryopreservation with antifreeze proteins: effect on gilthead seabream (*Sparus aurata*) plasma membrane lipids. Biol Reprod 2012; 86:59.
43. Zardoya R, Villalba S. A phylogenetic framework for the aquaporin family in eukaryotes. J Mol Evol 2001; 52:391–404.
44. Chen F, Lee Y, Jiang Y, Wang S, Peatman E, Abernathy J, Liu H, Liu S, Kucuktas H, Ke C, Liu Z. Identification and characterization of full-length cDNAs in channel catfish (*Ictalurus punctatus*) and blue catfish (*Ictalurus furcatus*). PLoS ONE 2010; 5:e11546.
45. Maricchiolo G, Genovese L, Laurà R, Micale V, Muglia U. Fine structure of spermatozoa in the gilthead sea bream (*Sparus aurata* Linnaeus, 1758) (Perciformes, Sparidae). Histol Histopathol 2007; 22:79–83.
46. Mulders SM, Preston GM, Deen PM, Guggino WB, van Os CH, Agre P. Water channel properties of major intrinsic protein of lens. J Biol Chem 1995; 270:9010–9016.
47. Tsukaguchi H, Weremowicz S, Morton CC, Hediger MA. Functional and molecular characterization of the human neutral solute channel aquaporin-9. Am J Physiol 1999; 277:F685–F696.
48. Litman T, Søgaard R, Zeuthen T. Ammonia and urea permeability of mammalian aquaporins. Handb Exp Pharmacol 2009; 190:327–358.
49. Ma T, Yang B, Verkman AS. Cloning of a novel water and urea-permeable aquaporin from mouse expressed strongly in colon, placenta, liver, and heart. Biochem Biophys Res Commun 1997; 240:324–328.
50. Liu K, Nagase H, Huang CG, Calamita G, Agre P. Purification and functional characterization of aquaporin-8. Biol Cell 2006; 98:153–161.
51. Koyama N, Ishibashi K, Kuwahara M, Inase N, Ichioka M, Sasaki S, Marumo F. Cloning and functional expression of human aquaporin8 cDNA and analysis of its gene. Genomics 1998; 54:169–172.
52. Engelund MB, Chauvigné F, Christensen BM, Finn RN, Cerdà J, Madsen SS. Differential expression and novel permeability properties of three aquaporin 8 paralogs from seawater-challenged Atlantic salmon smolts. J Exp Biol 2013; (in press). Published online ahead of print 18 July 2013; DOI 10.1242/jeb.087890.
53. Beitz E, Wu B, Holm LM, Schultz JE, Zeuthen T. Point mutations in the aromatic/arginine region in aquaporin 1 allow passage of urea, glycerol, ammonia, and protons. Proc Natl Acad Sci U S A 2006; 103:269–274.
54. Madsen SS, Olesen JH, Bedal K, Engelund MB, Velasco-Santamaria YM, Tipsmark CK. Functional characterization of water transport and cellular localization of three aquaporin parlogs in the salmonid intestine. Front Physiol 2011; 2:56.
55. Ikeda M, Andoo A, Shimono M, Takamatsu N, Taki A, Muta K, Matsushita W, Uechi T, Matsuzaki T, Kenmochi N, Takata K, Sasaki S, et al. The NPC motif of aquaporin-11, unlike the NPA motif of known aquaporins, is essential for full expression of molecular function. J Biol Chem 2011; 286:3342–3350.
56. Cutler CP, Harmon S, Walsh J, Birch K. Characterization of aquaporin 4 protein expression and localization in tissues of the dogfish (*Squalus acanthias*). Front Physiol 2012; 3:21.
57. Zapater C, Chauvigné F, Tingaud-Sequeira A, Finn RN, Cerdà J. Primary oocyte transcriptional activation of *aqp1ab* by the nuclear progestin receptor determines the pelagic egg phenotype of marine teleosts. Dev Biol 2013; 377:345–362.
58. Kagawa H, Kishi T, Gen K, Kazeto Y, Tosaka R, Matsubara H, Matsubara T, Sawaguchi S. Expression and localization of aquaporin 1b during oocyte development in the Japanese eel (*Anguilla japonica*). Reprod Biol Endocrinol 2011; 9:71.
59. Chaube R, Chauvigné F, Tingaud-Sequeira A, Joy KP, Acharjee A, Singh V, Cerdà J. Molecular and functional characterization of catfish (*Heteropneustes fossilis*) aquaporin-1b: changes in expression during ovarian development and hormone-induced follicular maturation. Gen Comp Endocrinol 2011; 170:162–171.
60. Sun Y, Zhang Q, Qi J, Chen Y, Zhong Q, Li C, Yu Y, Li S, Wang Z. Identification of differential genes in the ovary relative to the testis and their expression patterns in half-smooth tongue sole (*Cynoglossus semilaevis*). J Genet Genomics 2010; 37:137–145.
61. Nicchia GP, Frigeri A, Nico B, Ribatti D, Svelto M. Tissue distribution and membrane localization of aquaporin-9 water channel: evidence for sex-linked differences in liver. J Histochem Cytochem 2001; 49: 1547–1556.
62. Domeniconi RF, Orsi AM, Justulin LA Jr, Beu CC, Felisbino SL. Aquaporin 9 (AQP9) localization in the adult dog testis excurrent ducts by immunohistochemistry. Anat Rec (Hoboken) 2007; 290:1519–1525.
63. Ko SB, Uchida S, Naruse S, Kuwahara M, Ishibashi K, Marumo F, Hayakawa T, Sasaki S. Cloning and functional expression of rAOP9L a new member of aquaporin family from rat liver. Biochem Mol Biol Int 1999; 47:309–318.
64. Oliveira RL, Campolina-Silva GH, Nogueira JC, Mahecha GA, Oliveira CA. Differential expression and seasonal variation on aquaporins 1 and 9 in the male genital system of big fruit-eating bat *Artibeus lituratus*. Gen Comp Endocrinol 2013; 186C:116–125.
65. Tani T, Koyama Y, Nihei K, Hatakeyama S, Ohshiro K, Yoshida Y, Yaoita E, Sakai Y, Hatakeyama K, Yamamoto T. Immunolocalization of aquaporin-8 in rat digestive organs and testis. Arch Histol Cytol 2001; 64: 159–168.
66. Skowronski MT, Leska A, Robak A, Nielsen S. Immunolocalization of aquaporin-1, -5, and -7 in the avian testis and vas deferens. J Histochem Cytochem 2009; 57:915–922.
67. Coward K, Bromage NR, Hibbitt O, Parrington J. Gamete physiology and egg activation in teleost fish. Rev Fish Biol Fish 2002; 12:33–58.
68. Engel A, Fujiyoshi Y, Gonen T, Walz T. Junction-forming aquaporins. Curr Opin Struct Biol 2008; 18:229–235.
69. França LR, Hess RA, Cooke PS, Russell LD. Neonatal hypothyroidism causes delayed Sertoli cell maturation in rats treated with propylthiouracil: evidence that the Sertoli cell controls testis growth. Anat Rec 1995; 242: 57–69.
70. França LR, Russell LD. The testis of domestic animals. In: Martínez-García F, Regadera J (eds.), Male Reproduction: A Multidisciplinary Overview. Madrid: Churchill Communications; 1998:198–219.
71. Hermo L, Pelletier RM, Cyr DG, Smith CE. Surfing the wave, cycle, life history, and genes/proteins expressed by testicular germ cells. Part 4: intercellular bridges, mitochondria, nuclear envelope, apoptosis, ubiquitination, membrane/voltage-gated channels, methylation/acetylation, and transcription factors. Microsc Res Tech 2010; 73:364–408.
72. Bronson R. Biology of the male reproductive tract: its cellular and morphological considerations. Am J Reprod Immunol 2011; 65:212–219.
73. Lahnsteiner F. Morphology, fine structure, biochemistry, and function of the spermatic ducts in marine fish. Tissue Cell 2003; 35:363–373.
74. Cooper TG, Brooks DE. Entry of glycerol into the rat epididymis and its utilization by epididymal spermatozoa. J Reprod Fertil 1981; 61:163–169.
75. Mann T, White IG. Metabolism of glycerol, sorbitol and related compounds by spermatozoa. Nature 1956; 178:142–143.
76. Aalbers JG, Mann T, Polge C. Metabolism of boar semen in relation to sperm motility and survival. J Reprod Fertil 1961; 2:42–53.
77. Suzuki-Toyota F, Ishibashi K, Yuasa S. Immunohistochemical localization of a water channel, aquaporin 7 (AQP7), in the rat testis. Cell Tissue Res 1999; 295:279–285.
78. Ito J, Kawabe M, Ochiai H, Suzukamo C, Harada M, Mitsugi Y, Seita Y, Kashiwazaki N. Expression and immunodetection of aquaporin 1 (AQP1) in canine spermatozoa. Cryobiology 2008; 57:312–314.
79. Cosson J, Dreanno C, Billard R, Suquet M, Cibert C. Regulation of axonemal wave parameters of fish spermatozoa by ionic factors. In: Gagnon C (ed.), The Male Gamete: From Basic Knowledge to Clinical Applications. Montreal: Cache River Press; 1999:161–186.
80. Cosson J, Groison AL, Suquet M, Fauvel C, Dreanno C, Billard R. Studying sperm motility in marine fish: an overview on the state of the art. J Appl Ichthyol 2008; 24:460–486.
81. Abascal FJ, Cosson J, Fauvel C. Characterization of sperm motility in sea bass: the effect of heavy metals and physicochemical variables on sperm motility. J Fish Biol 2007; 70:509–522.
82. Yang B, Zhao D, Verkman AS. Evidence against functionally significant aquaporin expression in mitochondria. J Biol Chem 2006; 281: 16202–16206.
83. Sohara E, Ueda O, Tachibe T, Hani T, Jishage K, Rai T, Sasaki S, Uchida S. Morphologic and functional analysis of sperm and testes in aquaporin 7 knockout mice. Fertil Steril 2007; 87:671–676.
84. Calamita G, Ferri D, Gena P, Liquori GE, Cavalier A, Thomas D, Svelto M. The inner mitochondrial membrane has aquaporin-8 water channels and is highly permeable to water. J Biol Chem 2005; 280:17149–17153.
85. La Porta CA, Gena P, Gritti A, Fascio U, Svelto M, Calamita G. Adult murine CNS stem cells express aquaporin channels. Biol Cell 2006; 98: 89–94.
86. Lee WK, Bork U, Gholamrezaei F, Thévenod F. Cd(2+)-induced cytochrome c release in apoptotic proximal tubule cells: role of

mitochondrial permeability transition pore and Ca(2+) uniporter. Am J Physiol Renal Physiol 2005; 288:F27–F39.
87. Molinas SM, Trumper L, Marinelli RA. Mitochondrial aquaporin-8 in renal proximal tubule cells: evidence for a role in the response to metabolic acidosis. Am J Physiol Renal Physiol 2012; 303:F458–F466.
88. Saparov SM, Liu K, Agre P, Pohl P. Fast and selective ammonia transport by aquaporin-8. J Biol Chem 2007; 282:5296–5301.
89. Calamita G, Gena P, Meleleo D, Ferri D, Svelto M. Water permeability of rat liver mitochondria: a biophysical study. Biochim Biophys Acta 2006; 1758:1018–1024.
90. Soria LR, Fanelli E, Altamura N, Svelto M, Marinelli RA, Calamita G. Aquaporin-8-facilitated mitochondrial ammonia transport. Biochem Biophys Res Commun 2010; 393:217–221.
91. Bienert GP, Møller AL, Kristiansen KA, Schulz A, Møller IM, Schjoerring JK, Jahn TP. Specific aquaporins facilitate the diffusion of hydrogen peroxide across membranes. J Biol Chem 2007; 282:1183–1192.
92. Miller EW, Dickinson BC, Chang CJ. Aquaporin-3 mediates hydrogen peroxide uptake to regulate downstream intracellular signaling. Proc Natl Acad Sci U S A 2010; 107:15681–15686.
93. Dreanno C, Cosson J, Suquet M, Seguin F, Dorange G, Billard R. Nucleotide content, oxidative phosphorylation, morphology, and fertilizing capacity of turbot (*Psetta maxima*) spermatozoa during the motility period. Mol Reprod Dev 1999; 53:230–243.
94. Marchissio MJ, Francés DE, Carnovale CE, Marinelli RA. Mitochondrial aquaporin-8 knockdown in human hepatoma HepG2 cells causes ROS-induced mitochondrial depolarization and loss of viability. Toxicol Appl Pharmacol 2012; 264:246–254.